

1 Empirical stream thermal sensitivities cluster on the landscape 2 according to geology and climate

3 Lillian M. McGill¹, E. Ashley Steel², Aimee H. Fullerton³

4 ¹Center for Quantitative Sciences, University of Washington, Seattle, WA 98105, USA, ORCID ID: 0000-0003-2722-
5 2917

6 ²School of Aquatic and Fishery Sciences, University of Washington, Seattle, WA 98105, USA, ORCID ID: 0000-
7 0001-5091-276X

8 ³Northwest Fisheries Science Center, National Oceanic and Atmospheric Administration, 2725 Montlake Blvd. East,
9 Seattle, WA 98112, USA, ORCID 0000-0002-5581-3434

10 *Correspondence to:* Lillian M. McGill (lmcgill@uw.edu)

11 Abstract

12
13 Climate change is modifying river temperature regimes across the world. To apply management interventions in an
14 effective and efficient fashion, it is critical to both understand the underlying processes causing stream warming and
15 identify the streams most and least sensitive to environmental change. Empirical stream thermal sensitivity, defined
16 as the change in water temperature with a single degree change in air temperature, is a useful tool to characterize
17 historical stream temperature conditions and to predict how streams might respond to future climate warming. We
18 measured air and stream temperature across the Snoqualmie and Wenatchee basins, Washington during hydrologic
19 years 2015-2021. We used ordinary least squares regression to calculate seasonal summary metrics of thermal
20 sensitivity and time-varying coefficient models to derive continuous estimates of thermal sensitivity for each site. We
21 then applied classification approaches to determine unique thermal sensitivity regimes and, further, to establish a link
22 between environmental covariates and thermal sensitivity regime. We found a diversity of thermal sensitivity
23 responses across our basins that differed in both timing and magnitude of sensitivity. We also found that covariates
24 describing underlying geology and snowmelt were the most important in differentiating clusters. Our [findings and our](#)
25 [approach](#) can be used to inform strategies for river basin restoration and conservation in the context of climate change,
26 such as identifying climate insensitive areas of the basin that should be preserved and protected.

Deleted: findings

27 1 Introduction

28 Globally, river temperature regimes are shifting in response to a changing climate. As water temperature is a critical
29 component of aquatic ecosystems, these changes will alter an essential element of the habitat of many lotic organisms
30 (Daufresne and Boët 2007). To apply management interventions in an effective and efficient fashion, it is critical to
31 both understand the underlying processes causing stream warming (Arismendi et al. 2014, Steel et al. 2017) and
32 identify the streams most and least sensitive to environmental change (Parkinson et al. 2016, Pyne and Poff 2017,
33 Jackson et al. 2018). [Measures of empirical stream thermal sensitivity, defined as the change in water temperature](#)

35 with a single degree change in air temperature, or the slope of the statistical relationship between air temperature and
36 water temperature. address both concerns.

37 Thermal sensitivities reflect the combined influence of both spatially and temporally varying meteorological
38 and hydrological factors, and a large body of literature examines hypothesized climate, landscape, and hydrogeologic
39 drivers of thermal sensitivity (Table 1A). Variation in solar radiation is often the most important driver of both air and
40 river temperature, and as a result, air and river temperatures are typically correlated (Johnson 2003, Leach et al. 2023).
41 Landscape features such as riparian canopy cover and topographic shading associated with steep watersheds can
42 reduce exposure to solar radiation, suppressing stream temperatures (Webb and Zhang 1997). Stream temperature is
43 also influenced by discharge through changes to thermal inertia and residence time (Meier et al. 2003) and runoff
44 composition where snowmelt, surface runoff, or groundwater inflow entering the stream have different temperature
45 signatures than the stream itself (Webb and Zhang 1997, Mohseni and Stefan 1999, Cadbury et al. 2008). Inputs from
46 water sources such as snowmelt and groundwater upwelling decouple air and water temperatures and result in a
47 decreased thermal sensitivity of water temperature to air temperature (Tague et al. 2007, Mayer 2012, Johnson et al.
48 2014). As a result, the relationship between air and water temperature can also be a useful diagnostic tool for
49 identifying putative hydrological processes for which empirical measures are often unavailable. Thermal sensitivity
50 has been used in the past to estimate areas of shallow and deep groundwater influence (Snyder et al. 2015, Briggs et
51 al. 2018) and understand the role of snowmelt in modulating river temperature (Lisi et al. 2015, Winfree et al. 2018).
52 Despite conceptual agreement about hypothesized drivers of thermal sensitivity, substantial uncertainty persists
53 regarding the relative importance of these covariates in controlling and predicting thermal sensitivity.

54 Empirical stream thermal sensitivity has been widely used to characterize historical stream temperature
55 conditions and to predict how streams might respond to future climate warming (Mohseni et al. 2003, Mantua et al.
56 2010). Generally, larger thermal sensitivities indicate that water temperatures are more likely to track changes in air
57 temperature (Isaak et al. 2016, Mauger et al. 2017, Isaak et al. 2018b). However, there are concerns about using
58 current-day thermal sensitivities to predict future stream temperatures, as it can be difficult to derive insights about
59 river response to perturbations from statistical models that rely on historical relationships that may not extrapolate
60 well to future conditions. For example, past studies have found that using empirical relationships for extrapolating to
61 future climate scenarios without accounting for underlying processes such as snowmelt, groundwater, and annual
62 hysteresis may provide inaccurate predictions of future stream temperatures (Leach and Moore 2019, Steel et al. 2019).

Deleted: thermal sensitivity

Deleted: ¶

→ Both deterministic and statistical models have been used to study water temperature (Caissie 2006, Dugdale et al. 2017, Ouellet et al. 2020). Physical process-based models balance energy (heat) and mass (flow) fluxes in a water body (Glose et al. 2017). Process-based approaches allow the identification of the most important drivers in the heat budget of streams across timescales, improving the resolution and accuracy of stream temperature predictions (Stefan and Sinokrot 1993, van Beek et al. 2012, Wondzell et al. 2019). Issues exist with process-based modelling, however, including intensive data and computational needs (e.g., spatially distributed land use and soil characteristics, meteorological and discharge data, etc.), limited ability to generalize across basins, and difficulty representing groundwater and subsurface flow paths (Safieq et al. 2014). Statistical models are computationally simpler with potentially minimal data requirements (Benyahya et al. 2007) facilitating prediction at ecologically relevant spatial grains and extents. These models are appealing because of their simplicity and limited requirement of meteorological and hydraulic data, while still being characterized by high levels of explained variance in some basins. However, it can be difficult to derive insights about river response to perturbations from statistical models as statistical approaches rely on historical relationships that may not extrapolate well to future conditions. For example, relationships may change between water temperature and covariates such as discharge or the composition and coverage of riparian vegetation and land use. Statistical models would therefore benefit from a clearer understanding of the relationships between derived model coefficients and important watershed processes.

Deleted: Empirical stream thermal sensitivity, defined as the change in water temperature with a single degree change in air temperature, or the slope of the statistical relationship between air temperature and water temperature, has been widely used to characterize historical stream temperature conditions and to predict how streams might respond to future climate warming (Mohseni et al. 2003, Mantua et al. 2010).

Deleted: ew

Formatted: Font color: Black

Deleted: ;

Deleted: h

Deleted: employing this approach

Deleted: .

Deleted: .

Deleted: Pa

107 Under changing climatic conditions, the interrelations between air temperature and other processes controlling stream
108 temperature may not remain stable (Arismendi et al. 2014). Additionally, stream networks can exhibit patchy thermal
109 conditions due to spatially heterogeneous landscape attributes such as riparian shading, valley form and aspect, and
110 geology (Bogan et al. 2003, Benyahya et al. 2010). Large-scale models that do not incorporate fine-scale variation in
111 thermal sensitivity may not accurately predict thermal habitat at ecologically relevant scales. Despite these
112 shortcomings, thermal sensitivity remains a commonly used and straightforward tool that allows for comparison
113 between locations within rivers and has the potential to guide management.

114 There is a need to better understand how thermal sensitivities evolve throughout the year and along river
115 networks and to develop a clearer understanding of the relationships between derived model coefficients and important
116 watershed processes. Furthermore, thermal sensitivity itself can vary across time and space, rendering stationary
117 values insufficient to describe variability in this parameter. A clearer vision of how thermal sensitivities vary would
118 allow natural resource managers to understand what a single snapshot in time or space represents and could provide
119 insight into how river thermal sensitivity may evolve under nonstationary air temperature and precipitation regimes.
120 Groups of streams (clusters) that share similar patterns of thermal sensitivity will likely also share similar risk profiles.
121 Identification of stream clusters could help managers tailor investment in streams according to watershed-specific
122 influences (Mayer 2012). This study aims to answer three questions across two Pacific Northwest river basins: 1)
123 What is the spatial and temporal distribution of commonly used thermal sensitivity metrics across each basin? 2) What
124 are the representative thermal sensitivity regimes, how do they cluster on the landscape, and how do these clusters
125 differ from clusters based on air and water temperature individually? and 3) What are the landscape or climate factors
126 that best predict thermal sensitivity cluster membership? Finally, we consider the statistical functionality of these
127 methods on river networks.

128 2 Methods

129 2.1 Study Area

130 The Snoqualmie River begins as three distinct forks in the Mt. Baker Snoqualmie National Forest and drains a 1,813
131 km² watershed on the west side of the Cascade Range, Washington (Figure 1). The three forks originate in forested
132 public land before converging and flowing through a mix of agricultural, residential, and commercial land use. On
133 one major tributary, the Tolt River, a dam and a large reservoir provide drinking water for the City of Seattle (Figure

Deleted: ; hypothesized relationships are 1. **[use the rest of this paragraph to expand verbally some of our hypotheses]**
Despite conceptual agreement about hypothesized drivers of thermal sensitivity...

Deleted: the calculation of

Deleted: and

Deleted: c

Deleted: may be

Deleted: i

Deleted: ll

Deleted: Identification of g

Deleted: will also have management relevance. Groups of streams with similar thermal sensitivities

Deleted: ;

Deleted: may therefore

Deleted: within groups based on

Deleted:

Commented [AF3]: Not sure what this means to a novice reader. I'm thinking 7DadMax. Maybe just say 'thermal sensitivity'.

Deleted: air-water temperature

Commented [AF4]: Adjective to help here? Feels vague

Deleted: of air-water temperature correlations

Deleted: solely

Commented [HC5]: This is why I added the word in the abstract too – I think you have done so much statistical assessment that a small section in the discussion talking about the this approach in general is warranted and useful. So you found out some stuff about the SNo and Wen but also – this is as dense as a river monitoring network is likely to get and there are particular strengths and weaknesses of using this approach – such as specific results will always be susceptible to details of specific sites but general conclusions about drivers are pretty robust to specific sites and as more and more river networks “come on line” it will be possible to draw stronger and stronger conclusions about drivers more generally which is what will eventually be needed to refine hypotheses and/or use general results in a new place.

154 S4). The Wenatchee River drains 3,440 km² of the eastern Cascades before flowing into the Columbia River (Figure
155 S5). Although land use is similar to the Snoqualmie basin, wherein the headwaters originate in forested public lands
156 before flowing through a mix of agricultural, residential, and commercial land use, forest density is generally lower
157 in the eastern Cascades.

158 Both the Snoqualmie and Wenatchee basins have a Mediterranean climate with dry summers and wet, mild
159 winters influenced by proximity to the Pacific Ocean. The climate on the east side of the Cascades is drier than that
160 of the west side; ~~the average annual precipitation is 1874 mm (939 mm), and the average annual temperature is 5.7°C~~
161 ~~(5.3°C) for the western (eastern) Cascades.~~ However, the prevailing westerly winds, which cross the Cascades, create
162 temperature and precipitation gradients that vary widely across the Wenatchee basin. ~~In both basins,~~ precipitation
163 occurs predominately from October to March. The coldest month is typically January, whereas the warmest is July.
164 Rivers have a mixed rain-snow hydrology with substantial winter rain and spring snowmelt, although the Wenatchee
165 basin receives ~~more~~ winter precipitation as snow. Peak flow generally occurs during winter in the Snoqualmie River
166 and spring in the Wenatchee River (Figure 2). ~~Geology differs across the basins. Geology of the Snoqualmie basin is~~
167 ~~characterized by a deep glacial aquifer in the lowland portion of the watershed, whereas in the alpine area much of the~~
168 ~~ground surface is directly underlain by bedrock that lacks significant fracture systems (Turney et al. 1995, Bethel~~
169 ~~2004). In contrast, the Wenatchee basin's geology consists of both an aquifer within the sedimentary bedrock of the~~
170 ~~central and lowland areas and an overlying unconsolidated alluvial and outwash aquifer located primarily in river~~
171 ~~valley bottoms (Montgomery Water Group 2003).~~ The Snoqualmie and Wenatchee basins both have reaches where
172 water temperature exceeds regulatory thresholds established for salmonids that are protected by the U.S. Endangered
173 Species Act (ESA). Both basins support ESA-listed Chinook Salmon (*Oncorhynchus tshawytscha*) and Steelhead
174 Trout (*Oncorhynchus mykiss*) and the Wenatchee basin additionally supports populations of Bull Trout (*Salvelinus*
175 *confluentus*) and Sockeye Salmon (*Oncorhynchus nerka*).

176 Water temperature loggers ($N_{\text{Snoqualmie}}=42$, $N_{\text{Wenatchee}}=31$) were installed throughout the mainstems, on major
177 tributaries and on a selection of minor tributaries for both the Snoqualmie and Wenatchee rivers (Figure 1). Practical
178 limitations forced sites to be publicly accessible, or on private property with landowner permission, and within 1 km
179 of a road. For this study, water temperature was recorded using HOBO TidbiT v2 (UTBI-001) loggers every hour
180 from October 1, 2014 through September 30, 2021 in both basins. We hereafter use North American hydrologic years
181 (1 October – 30 September) instead of calendar years with the year of summer data as the year of reference. Air

Moved (insertion) [1]

Deleted: T

Deleted: long-term

Deleted: was

Deleted: for the western (eastern) Cascade

Deleted: s time series

Deleted: ¶

Deleted: h

Deleted: P

Deleted: a greater proportion of

191 temperature data was recorded using HOBO Pendant (UA-002-64) loggers every hour at all water temperature
192 monitoring sites. Air temperature was logged for subset of 11 (6) sites in the Snoqualmie (Wenatchee) basin beginning
193 October 1, 2014, and for all sites beginning October 1, 2016 (October 1, 2018). Air loggers were placed on trees along
194 the stream bank, as close to the stream temperature loggers as possible. The air temperature loggers were secured at
195 approximately breast height on the north side of the trees. Solar shields were fashioned to house both water and air
196 temperature loggers.

197 **2.2 Exploratory analysis of air-water correlation summary metrics**

198 We calculated two summary metrics to characterize the relationship between air temperature and water temperature.
199 For each site, summary metrics were derived from linear regressions between mean daily values of air and water
200 temperature. The slope of this relationship, the thermal sensitivity, indicates the average difference in water
201 temperature when comparing time periods with a one-degree difference in air temperature. For example, a thermal
202 sensitivity of 0.5 would indicate that, based on historical data, when air temperature at a site differs by 1°C, water
203 temperature differs on average by 0.5°C (Leach and Moore 2019). The strength of this relationship (R^2) is an indicator
204 of how well water temperature can be approximated by air temperature and is calculated as the Pearson correlation
205 value between air and water temperature. Summary metrics were calculated separately for each season. Seasons were
206 defined as fall (October, November, December), winter (January, February, March), spring (April, May, June), and
207 summer (July, August, September).

208 Watersheds for each site were delineated and covariates describing the watersheds were obtained from
209 commonly available geostatistical products (Table 2). Covariates were divided into four broad categories: basin
210 topography (watershed area, mean watershed elevation, average stream slope, and distance upstream), land use
211 (percent watershed forest, riparian forest, and lake area), climate (average temperature, precipitation, and percent
212 precipitation falling as snow), and hydrogeologic (baseflow index, hydraulic conductivity, and soil depth to bedrock).
213 Temperature, precipitation, and percent precipitation as snow were obtained from DAYMET Daily Surface Weather
214 data (Thornton et al. 2020) and all other landscape covariates were obtained from the Stream-Catchment (StreamCat)
215 Database (Hill et al. 2016).

216 A large body of literature examines landscape-level drivers of air and water temperature correlations within
217 rivers. Therefore, we first summarized hypothesized drivers of thermal sensitivity based on previous literature and
218 their covarying landscape variables within our basins (Table 1A). We then conducted an exploratory analysis of the

219 relationship between landscape covariates and thermal sensitivity to better understand patterns in our data and set up
220 future hypothesis testing. Due to the correlated nature of our dataset, no formal statistical tests were conducted. We
221 plotted summer thermal sensitivity against hypothesized drivers, including mean watershed elevation (MWE),
222 watershed slope, distance upstream, percent riparian forest cover, and substrate hydraulic conductivity. Loess curves
223 were plotted to aid in data visualization, and correlation coefficients between thermal sensitivity and each landscape
224 covariate were used to quantify the strength of the linear relationship.

Deleted: Covariate descriptions and sources are found in Table 1.
(Hill et al. 2016)

225 We also explored the relationship between spring thermal sensitivity and snowmelt, defined as the change in
226 Snow Water Equivalent (SWE) for a given season and denoted as ΔSWE , and between summer thermal sensitivity
227 and mean air temperature and total precipitation. Climatic variables were obtained from gridded DAYMET data
228 products (Thornton, et al. 2020) and calculated for the upstream catchment of each monitoring station.

Deleted: M.M.

229 2.3 Spatially weighted clustering of thermal sensitivity, water temperature, and air temperature

230 To identify representative regimes of air-water temperature correlations, we employed a varying-coefficient linear
231 model to obtain continuous, daily estimates of thermal sensitivity. We then defined a spatially weighted dissimilarity
232 matrix for use in clustering, which quantifies the spatial correlation in thermal sensitivity time series while accounting
233 for the directed river network structure. We used this spatially weighted dissimilarity matrix with agglomerative
234 hierarchical clustering to identify groups of sites exhibiting similar patterns in thermal sensitivity over time and
235 compared these clusters to those generated using only water or air temperature. Details of each step are provided in
236 the following sections.

237 2.3.1 Varying coefficient linear model for air-water relationship

238 To derive a continuous thermal sensitivity metric, we fit a time-varying coefficient model (TVCM) to air and water
239 temperature data. The TVCM is an effective tool for exploring dynamic features of the sensitivity of water temperature
240 with changes in air temperature and uses a parametric linear model but with time-varying coefficients (Li et al. 2014,
241 2016). For a given site, we described the varying coefficient model for the air–water temperature relationship as:

$$242 \quad y_t = \beta_{0,t} + x_t \beta_{1,t} + \epsilon_t, t = 1, \dots, T \quad (1)$$

243 Where $\beta_{0,t}$ and $\beta_{1,t}$ are varying intercept and slope coefficients. To estimate the time-varying coefficients, we adopted
244 an ordinary least squares kernel regression with the Nadaraya–Watson estimator, where we fit a set of weighted local
245 regressions with an optimally chosen window size defined by the bandwidth, b , and the weights given by the kernel

249 function (Hoover 1998, Casas and Fernandez-Casal 2019). The kernel and its bandwidth control the level of smoothing
250 by adjusting the weight that the neighbouring time points have on estimates at t . The bandwidth was set to 0.2 a priori
251 to ensure consistency across time series. We used the Gaussian kernel that is of the form $k(x) = \frac{1}{2}\pi e^{-\frac{x^2}{2}}$. The varying
252 intercept term represents the mean water temperature at time t and the varying slope term represents the local
253 sensitivity of water temperature to changes in air temperature at time t . We used the R package tvReg (Casas and
254 Fernandez-Casal 2021) for implementing the model.

255 We filtered resultant time series for site-years with > 218 days (60% of the year) and gaps of ≤ 7 days,
256 yielding 250 site-years from 74 sites across both the Snoqualmie and Wenatchee basins. To capture the typical range
257 and timing of thermal sensitivity at each site, we created a single representative time series of thermal sensitivity at
258 each site by calculating the mean daily thermal sensitivity for each day of the year across all years of filtered data. We
259 use this average annual time series for subsequent clustering analyses. To ensure that using an average annual time
260 series of thermal sensitivity was an appropriate choice given the structure of our data, we conducted a supplementary
261 analysis to assess cluster sensitivity to interannual variability (Appendix A). [Measured air and water temperature and
262 modelled thermal sensitivities can be visualized at the following link:
263 \[https://lmcgill.shinyapps.io/TimeVarying_AWC/\]\(https://lmcgill.shinyapps.io/TimeVarying_AWC/\).](https://lmcgill.shinyapps.io/TimeVarying_AWC/)

264 2.3.2 Estimating a spatially weighted dissimilarity matrix

265 To quantify spatial correlation while accounting for the directed river network structure, we developed a dissimilarity
266 measure for time series of thermal sensitivity, water temperature, and air temperature that incorporated spatial
267 correlation between sites (Haggarty et al. 2015). The general form of the proposed dissimilarity measure between sites
268 x and y can be written as:

$$269 \quad d_{xy}^c = d_{xy} \text{cov}(h_s) \quad (2)$$

270 where d_{xy}^c is the spatially weighted dissimilarity matrix, d_{xy} is the Canberra distance (Lance and Williams 1967), and
271 $\text{cov}(h_s)$ is a valid stream distance-based covariance matrix.

272 To estimate $\text{cov}(h_s)$, we used the tail-down model that was introduced by Ver Hoef and Peterson (2010).
273 Due to the complex structure of the tail-down model, it is necessary to model spatial correlation on a river network
274 with a covariogram. We first estimated the covariance between time series at each site using a classic formula from
275 Cressie (1993), which states that the estimated covariance between sites x and y is given by

276
$$cov(x, y) = \sum_{t=1}^T \frac{\{x_t - \bar{x}\}\{y_t - \bar{y}\}}{T} \quad (3)$$

277 where x_t and y_t are the values of the variable (thermal sensitivity, water temperature, or air temperature) at sites x and
 278 y at time t and T is the total number of discrete times. This results in a single value which summarizes the covariance
 279 between the time series at the two sites over the period of interest. We then plotted these point summaries of the
 280 covariance between pairs of curves against lags (measured as stream distance) to obtain an empirical stream distance-
 281 based covariogram. We fit an exponential covariance function to this empirical covariogram and evaluated the model
 282 at relevant distances to obtain an estimated stream distance-based covariance matrix $cov(h_s)$. We used this new
 283 covariance matrix to weight the Canberra distance matrix as shown in Equation 2. The final spatially weighted
 284 dissimilarity matrix, d_{xy}^c , was then used in clustering analyses.

285 **2.3.3 Agglomerative hierarchical clustering**

286 We used agglomerative hierarchical clustering (AHC) to identify groups of sites where the patterns in thermal
 287 sensitivity, water temperature, and air temperature were similar over time using the `hclust` function in R (R Core Team
 288 2020). AHC is a common clustering method (Olden et al. 2012, Maheu et al. 2016, Savoy et al. 2019, Isaak et al.
 289 2020) where each time series starts in its own cluster, and the hierarchy is built by repeatedly merging pairs of similar
 290 clusters separated by the shortest distance (i.e., measured as the similarity between individual times series) until all
 291 points are contained in a single cluster. To decide which clusters are merged in every iteration, AHC uses a dissimilarity
 292 metric (d_{xy}^c , derived in Equation 2) and a linkage criterion. We used Ward’s minimum variance linkage method for
 293 clustering, where the distance between two clusters is computed as the increase in the sum of squared differences after
 294 combining two clusters into a single cluster. The shortest of these links (minimum increase in the sum of squared
 295 differences) that remains at any step causes the fusion of the two clusters whose elements are involved.

296 A difficulty associated with cluster analysis is determining the most appropriate number of clusters given the
 297 data because no a priori optimal number of clusters exists. Clusters resulting from alternative choices can be evaluated
 298 through internal cluster validity indices (CVI); there are a variety of CVIs, most of which combine within cluster
 299 cohesion (intra-cluster variance) or between cluster separation (inter-cluster variance) to compute a quality measure.
 300 There is no universally best CVI (Arbelaitz et al. 2013), therefore we calculated a suite of five CVIs, including the
 301 Silhouette, Gap, Davies–Bouldin, Calinski–Harabasz, and generalized Dunn indices, using the `NbClust` R package

302 (Charrad et al. 2014). A final number of clusters was determined by a majority rules approach based on the optimal
303 number of clusters suggested by each index (Table S2).

304 To determine whether clusters assignment were stable, or preserved under a perturbed dataset similar to the
305 original and therefore likely reflective of real differences, we conducted a bootstrapping approach where sites were
306 sampled with replacement and then AHC was performed on the resampled data using the fpc R package (Hennig
307 2020). For each bootstrapped cluster, we assessed the similarity between each new cluster and the most similar original
308 cluster with the Jaccard index. The Jaccard coefficient ranges from 0 to 1. Clusters with a coefficient larger than 0.75
309 were considered stable, clusters with a coefficient between 0.5 and 0.75 indicate that the cluster is measuring a pattern
310 in the data but exact site assignment may be doubtful, and clusters with a mean Jaccard coefficient of less than 0.5
311 were considered unstable and may not reflect a true pattern in the data (Maheu et al. 2016, Savoy et al. 2019). We
312 repeated the bootstrapping procedure 10,000 times; the mean Jaccard coefficient for each cluster is reported in Table
313 4.

314 2.3.4 Identification of environmental drivers in thermal sensitivity

315 We used classification and regression trees (CART; Breiman et al. 1984) to investigate the relative importance of
316 hydrogeologic, climatic, landscape, and basin topography attributes for predicting each site's membership to a thermal
317 sensitivity cluster. CART is typically used to attempt to predict membership to clusters using environmental attributes,
318 and it allows the modelling of nonlinear relationships among mixed variable types and facilitates the examination of
319 intercorrelated variables in the final model (De'ath and Fabricius 2000, Olden et al. 2008). We took an exploratory
320 approach to this analysis due to our relatively small sample size ($N_{\text{Snoqualmie}} = 42$, $N_{\text{Wenatchee}} = 31$), which limited our
321 ability to conduct statistical tests. Therefore, we calculated variable relative importance, defined as the sum of squared
322 improvements at all splits determined by the predictor. These values are scaled to sum to 100 (rounded). To ensure no
323 single site unduly impacted CART results (Krzywinski and Altman 2017), we conducted a supplementary leave-one-
324 out-cross-validation analysis to ensure relative importance estimates were stable across different permutations of the
325 data (Figure S7). We used the R package rpart (Therneau and Atkinson 2019) for implementing the CART model.
326 Covariates examined are described in Table 2.

Deleted: physical drainage basin

Deleted: 1

329 **3 Results**

330 **3.1 General patterns in temperature, precipitation, and thermal sensitivity**

331 This analysis included data from seven hydrologic years, each with differing temperature and precipitation patterns.
332 Generally, the years spanned by our dataset were warmer than the historical average (1901-2000), with wetter than
333 average winter and fall months and drier spring and summer months (Figure S1). For the western (eastern) Cascades,
334 all years (2015-2021) have average annual temperatures higher than the long-term average of 8.6 °C (3 °C), although
335 individual seasons were slightly cooler than average. The year 2015 stood out as a year with an exceptionally warm
336 winter, low snowpack, and dry spring. Temperature and precipitation patterns in the western and eastern Cascades
337 were generally similar, however, precipitation anomalies were typically smaller in the eastern Cascades due to the
338 overall lower precipitation in this region (Figure 2; Figure S1).

339 Summary metrics describing air-water temperature relationships exhibited substantial variation across time
340 (season and year) and space. Across all season-year combinations, thermal sensitivities ranged from 0.05 to 0.97
341 (mean = 0.54) in the Snoqualmie basin and from 0.06 to 0.74 (mean = 0.42) in the Wenatchee basin (Table 3). Seasonal
342 distributions of thermal sensitivities differed. For example, fall thermal sensitivities were relatively homogeneous,
343 with 90% of values falling between 0.47 and 0.70, whereas spring and summer thermal sensitivities exhibited a broader
344 range of values, with 90% of values falling between 0.30 and 0.84 in spring and 0.25 and 0.78 in summer. Air
345 temperature was generally a good predictor of water temperature, as evidenced by R² values that ranged from 0.20 to
346 0.99 (mean = 0.88) in the Snoqualmie basin and from 0.08 to 0.98 (mean = 0.85) in the Wenatchee basin (Table 3).

347 Overall, weak and inconsistent patterns emerge in summer between thermal sensitivity and landscape and
348 climate variables (Figure 3; Table 1B). For climate variables, only ASWE appeared to have a linear relationship with
349 thermal sensitivity (Figure 3). The relationship between ASWE and thermal sensitivity was negative and non-linear,
350 displaying a wedge-shaped pattern wherein large snowmelt events did not reduce thermal sensitivities below 0.25
351 (Figure 3). For landscape variables, correlation coefficients were overall small ($|\rho| < 0.3$), indicating weak to non-
352 existent linear relationships between landscape covariates and observed thermal sensitivity (Table 1B). A weakly
353 negative relationship between thermal sensitivity and distance upstream was observed for both basins. Percent riparian
354 forests and thermal sensitivity showed no relationship for either basin. The relationship between hydraulic
355 conductivity and thermal sensitivity was weakly positive and parabolic in the Snoqualmie basin.

Moved up [1]: The long-term average annual precipitation was 1874 mm (939 mm) for the western (eastern) Cascades time series.

Deleted: Table 2

Deleted: Table 2

Deleted: Table 3

Deleted: SWE

Deleted: SWE

Deleted: Table 3

364 **3.2 Patterns of clustering for water temperatures, air temperatures, and thermal sensitivities**

365 Time-varying thermal sensitivities displayed periods of both high and low values within a season, which was not
366 necessarily represented when looking only at seasonal summary metrics (Figure 4 and Figure 5). Thermal sensitivity
367 varied alongside water and air temperature within the Snoqualmie and Wenatchee basins. Generally, thermal
368 sensitivity rose sharply in late spring, was highest in late summer, declined slowly throughout the fall, and remained
369 depressed through winter and early spring.

370 Spatially weighted AHC yielded four clusters for thermal sensitivity, with a cluster validity index (CVI)
371 range of 2-4, and two clusters each for air (CVI range of 2-5) and water (CVI range of 2-4) temperature in the
372 Snoqualmie basin, and five clusters for thermal sensitivity (CVI range 2-5) and two clusters each for air (CVI range
373 of 2-3) and water (CVI range of 2-5) temperature in the Wenatchee basin (Figure 4; Figure 5; Table S2). For both
374 basins, clusters of air and water temperature correspond closely with elevational gradients (Figure S4; Figure S5).
375 Higher elevation sites exhibited generally lower magnitudes but similar patterns in air and water temperatures (Table
376 4). For example, within both basins seasonal water temperatures were synchronized, with the cluster minimum and
377 maximum water temperatures occurring within a day of each other (Table 4). In the Snoqualmie basin, air temperature
378 clusters were stable, with a mean Jaccard index of 0.91 for high elevation sites (Cluster 2, [n=11 sites](#)) and 0.73 for
379 low elevation sites (Cluster 1, [n=31 sites](#)). Water temperature clusters were slightly less stable, with a mean Jaccard
380 index of 0.65 for high elevation sites (Cluster 2, [n=17 sites](#)) and 0.89 for low elevation sites (Cluster 1, [n=25 sites](#)).
381 Air and water temperature clusters in the Wenatchee basin were more stable than the Snoqualmie clusters. In the
382 Wenatchee basin, air temperature clusters had a mean Jaccard index of 0.85 for high elevation sites (Cluster 2, [n=25](#)
383 [sites](#)) and 0.95 for low elevation sites (Cluster 1, [n=6 sites](#)), and water temperature clusters had a mean Jaccard index
384 of 0.86 for high elevation sites (Cluster 2, [n=23 sites](#)) and 0.73 for low elevation sites (Cluster 1, [n=8 sites](#)).

385 Clustering patterns for thermal sensitivity were more complex and less stable than air and water temperature
386 clusters, particularly for the Snoqualmie basin (Figure 4; Figure 5; Table 4). In the Snoqualmie basin, Cluster 1 ([n=11](#)
387 [sites](#)) consisted primarily of low elevation tributaries that exhibited stable thermal sensitivities throughout the year,
388 producing a cluster-average range of only 0.15 (Figure 4; Table 4). Cluster 2 was small ([n=5 sites](#)), and the distribution
389 of sites within this cluster included three mainstem sites and two high elevation tributaries. Despite the large
390 geographic distances separating sites, this cluster was highly stable with a mean Jaccard index of 0.88. Cluster 2 was
391 characterized by a mean thermal sensitivity of 0.52 and the highest annual variability, with a cluster-average range of

Deleted: (water)

Deleted: (0.86)

Deleted: (0.73)

Deleted: .

396 0.45. Cluster 3 was large (n=15 [sites](#)) and contained sites located within the upper regions of the Snoqualmie River.
397 Cluster 3 had the lowest mean thermal sensitivity (mean=0.40). Lastly, Cluster 4 ([n=11 sites](#)) exhibited the lowest
398 stability of any cluster in the Snoqualmie basin, with a mean Jaccard index of 0.55. Sites in this cluster were mainly
399 situated on the mainstem Snoqualmie and its major tributaries. This cluster was distinguished by the highest mean
400 thermal sensitivity (mean=0.65). In the Wenatchee basin, all five thermal sensitivity clusters were relatively stable.
401 Clusters 1 ([n=7 sites](#)), 4 ([n=8 sites](#)), and 5 ([n=8 sites](#)) demonstrated similar seasonal patterns in thermal sensitivities,
402 with minimum values occurring in late Spring (water days 216, 207, 214) and maximum values occurring in late
403 summer (water days 324, 331, 330). These clusters also showed moderate to high stability (mean Jaccard indices of
404 0.79, 0.86, and 0.79). Cluster 3 ([n=7 sites](#)) exhibited the highest mean thermal sensitivity (mean=0.40) and
405 encompassed primarily low elevation tributaries (Peshastin and Mission Creek; Figure S5). Cluster 2 was unique in
406 that it consisted of a single site (Chumstick Creek) that was nearly always assigned to a unique cluster when included
407 in the bootstrapping procedure. The thermal sensitivity for this site was low (mean=0.29) and virtually flat throughout
408 the year (range = 0.07).

409 CART analysis indicated that basin topography and hydrogeology were the principal discriminators of
410 thermal sensitivity clusters. The top predictors of cluster membership (i.e., predictors with a greater than 10% increase
411 in mean standard error if removed from the model) were MWE and baseflow index in the Wenatchee basin and
412 watershed slope, MWE, and soil depth in the Snoqualmie basin (Figure 6). Variable importance distributions differed
413 between the Wenatchee and Snoqualmie basins, although in both basins several covariates had similar relative
414 importance values. Covariate distributions also varied across clusters within a basin. In the Snoqualmie basin, Cluster
415 1 sites were generally below a MWE of 600 meters, whereas Cluster 3 sites were generally mid-sized and high
416 elevation with a low baseflow index. In the Wenatchee basin, Cluster 1, 4, and 5 sites were predominately located at
417 high elevations with steep slopes. Cluster 4 sites exhibited a large proportion of precipitation falling as rain. Sites in
418 Clusters 2 and 3 were generally low elevation sites with a high baseflow index and soil depth.

419 **4 Discussion**

420 Thermal sensitivity varies throughout the year and reflects hydrologic conditions at a given time and place within a
421 watershed; therefore, it should not be conceptualized as a static value. Although summary metrics of thermal
422 sensitivity, such as average values over the summer, can still prove useful and informative, it is essential to

423 acknowledge the non-stationarity of the relationship between air and water temperature to obtain an accurate
424 understanding of how river temperature responds to changing conditions. We find that underlying geology and climate
425 are important controls on thermal sensitivity across two Pacific Northwest river basins, and thermal sensitivities reflect
426 aspects of river dynamics not redundant with water and air temperature. Overall, this study provides a framework for
427 using thermal sensitivity regimes to improve understanding of factors contributing to stream temperatures and will
428 enable managers to target mitigation and adaptation activities to work best with local conditions within a watershed.

Deleted: U

Deleted:

429 **4.1 Patterns of thermal sensitivity clustering**

430 Our analysis of stream air and water temperatures supports the presence of distinct thermal sensitivity regimes,
431 providing an organizing framework for river research and management by identifying sites with similarities across the
432 network. We found that thermal sensitivity regimes reflected non-redundant aspects of river dynamics relative to air
433 and water temperature alone. Air temperature and water temperature clusters closely corresponded to one another and
434 were almost entirely determined by elevation of the temperature loggers, whereas thermal sensitivity clusters showed
435 more variability in annual patterns and were intermixed spatially (Figure 4; Figure 5). Previous studies within the
436 Pacific Northwest found that, generally, colder streams are less sensitive to air temperature fluctuations than warmer
437 streams (Luce et al. 2014, Kelleher et al. 2021). Air and water clustering results are consistent with previous studies
438 that observed broad temporal correspondence of air and river temperature dynamics with differing magnitudes of
439 response (Bower et al. 2004, Chu et al. 2010, Garner et al. 2014, Isaak et al. 2018a). More locally, Isaak et al. (2020)
440 found that across western rivers, much of the information in stream temperature records could be summarized by a
441 relatively limited number of distinct regime components primarily driven by differences in elevation and latitude.

Deleted: (

442 Viewing thermal sensitivity as a continuous parameter adds novel insights to our understanding of river basin
443 functioning. Studies have highlighted the importance of annual shifts in the processes that drive heat budgets as well
444 as the non-stationarity of the resulting statistical relationships (Arismendi et al. 2014, Boyer et al. 2021). Our clustering
445 analysis overcomes these issues by using a varying coefficient model that treats thermal sensitivity as a continuous
446 function through time, rather than a series of discrete summary metrics, and allows clustering based on the entirety of
447 average annual patterns. The observed complexity in thermal sensitivity response hints at the diversity of physical
448 processes controlling stream temperature response and the large, clear shifts in thermal sensitivity magnitude across
449 the year calls into question the common practice of summarizing a river's sensitivity as a static value. The ability to
450 directly observe shifts in the air-water temperature relationships also opens the possibility of using thermal sensitivity

454 as a diagnostic tool to examine gradual changes in the importance of drivers of water temperature, such as dynamic
455 changes in riparian shading or snowmelt.

456 **4.2 Climate controls on thermal sensitivity**

457 Seasonal variability of thermal sensitivity metrics was evident for our basins. Within both the Snoqualmie and
458 Wenatchee basins, winter thermal sensitivities were low and varied strongly with MWE (Figure 1). Observed low
459 thermal sensitivities in winter were likely due to the non-linear relationship between air and stream temperature at
460 cold temperatures when air temperatures can dip below the water temperature-freezing limit (Mohseni et al. 1998,
461 1999). Air temperature covaries strongly with elevation in Pacific Northwest basins, and sites that are high in the
462 watershed will experience a greater number of sub-freezing days, and therefore greater decoupling between air and
463 water temperatures. Fall thermal sensitivities were relatively homogeneous whereas spring and summer thermal
464 sensitivities exhibited a broader range of values. We expect thermal sensitivities to be similar during periods of heavy
465 precipitation, when water sources with thermal characteristics distinct from air temperature, such as groundwater and
466 snowmelt, contribute relatively less flow. The greater variability of responses in spring and summer indicates that the
467 [relative magnitude of energy exchange](#) processes controlling river temperatures are more diverse than in fall or winter
468 (Hrachowitz et al. 2010).

469 Snowmelt likely contributed to observed differences in thermal sensitivity across sites in spring and early
470 summer. For summary metrics, the relationship between snowmelt and spring thermal sensitivity formed a wedge-
471 shaped pattern, wherein sites with limited snowmelt displayed both high and low thermal sensitivity, but sites with
472 extensive snowmelt always display low thermal sensitivity (Figure 3). For the clustering analysis, although the
473 proportion of precipitation falling as snow showed limited variable importance, MWE and slope covaried closely with
474 snow accumulation and were among the most important predictors of cluster membership, perhaps masking a
475 statistical signal of snowfall (Figure 6). In both the Snoqualmie and Wenatchee basins, clusters with higher elevation,
476 steeper slope, and greater snowmelt within the catchment had thermal regimes that were less sensitive to changes in
477 air temperature during spring and early summer. Importantly, snowmelt buffering, the process wherein snowmelt-
478 influenced streams have lower thermal sensitivity due to a direct input of cold water and a corresponding increase in
479 flow rates and water depths (van Vliet et al. 2011, Siegel et al. 2022), diminishes throughout the summer. By late
480 summer, high elevation, snowmelt influenced sites were often more sensitive to air temperatures than their low
481 elevation counterparts (Figure 4; Figure 5). Sites within Cluster 4 in the Wenatchee basin were an exception to this

482 pattern and maintained summer thermal sensitivities that were substantially depressed relative to adjacent locations
483 (e.g., Clusters 1 and 5). This is likely due to snowmelt inputs within these catchments, and points to the importance
484 of high elevation, late-summer snowpack melt as a significant source of summer baseflow and control on water
485 temperatures during the months of greatest heating within these watersheds.

Deleted: glacial

Deleted: glacial and

486 Numerous studies have examined the buffering impact of snowmelt on water temperature due to advective
487 flux from cooler meltwater entering the river. Studies in Alaskan rivers found a linear, negative relationship between
488 summer thermal sensitivity and snowmelt (Lisi et al. 2015, Cline et al. 2020) and a recent study in the Snoqualmie
489 basin found that snowmelt can reduce basin-wide peak summer temperatures, particularly at high elevation tributaries,
490 and the thermal impacts of melt water can persist through the summer (Yan et al. 2021). Our results suggest that
491 snowpack offers substantial buffering to changes in air temperature across mountain river basins, but that the largest
492 impacts are localized across space and time. Climate change is expected to shift snowmelt earlier and reduce snow
493 water resources (Barnett et al. 2005, Musselman et al. 2021). The loss of snow may result in warming in snow-
494 influenced systems and the subsequent homogenization of thermal conditions across basins (Winfree et al. 2018).
495 Homogenization of thermal conditions likely leads to important changes in ecological functions and ecosystem
496 services supported by lost thermal heterogeneity, such as a loss of cold-water patches for Pacific salmon (Brennan et
497 al. 2019).

498 **4.3 Hydrogeologic controls on thermal sensitivity**

Deleted: G

499 Hydrogeologic characteristics shaped the relationship between air and water temperatures across the Wenatchee and
500 Snoqualmie basins. The inclusion of baseflow index, hydraulic conductivity, and soil depth in determining cluster
501 membership (Figure 6) implies the importance, and detectability, of groundwater as a key mediator of thermal
502 sensitivity regimes in Pacific Northwest basins. Clusters with high baseflow index, hydraulic conductivity, and soil
503 depth values generally had lower summer and less variable thermal sensitivities (Figure 4; Figure 5; Figure 6),
504 implying greater groundwater influence (Kelleher et al. 2012). Interestingly, despite the clear importance of
505 hydrogeologic metrics in the clustering analysis, results from summary metric exploratory analysis were mixed and,
506 in the Snoqualmie basin, did not align with expectations of a negative relationship between thermal sensitivity and
507 groundwater influence (Table 1B). Although it is possible to infer broad patterns in surface-groundwater connectivity
508 using datasets of interpolated geologic properties (i.e., hydraulic conductivity, soil depth) or water source (i.e.,
509 baseflow index), individual hydrogeologic metrics often have substantial uncertainty, do not covary perfectly, and

Deleted: Geologic

Deleted: groundwater

Deleted: Table 3

Deleted: hydrogeologic

517 may be particularly unconstrained for mountain headwater streams (Wolock et al. 2004, Patton et al. 2018, Briggs et
518 al. 2022). Additionally, the influence of these processes can be localized and variable across space (Johnson et al.
519 2017) and substantially impacted by human modification. The ability to use thermal sensitivity as an empirical
520 measure of groundwater influence, therefore, shows great promise for understanding catchment processes and
521 informing management and restoration actions at ecologically relevant scales (Snyder et al. 2015). Although our
522 approach moves us closer to a mechanistic understanding of the relationship between thermal sensitivity and
523 groundwater, mixed results from our analyses emphasize the need for additional targeted studies.▼

Deleted: .

524 An investigation of the underlying geology across the Snoqualmie and Wenatchee basins supports our
525 conclusion that low thermal sensitivities are indicative of groundwater inputs. The lowland portion of the Snoqualmie
526 watershed contains a deep, permeable, productive glacial aquifer that is presumed to be the source of summer baseflow
527 to much of the river (Bethel 2004, McGill et al. 2021, Turney et al. 1995). Glacial and interglacial deposits in the
528 valley contain several geohydrologic units with differing aquifer potential (Bethel 2004); however, most deposits can
529 form small but useable aquifers that could be helping to sustain baseflow in summer months (Turney et al. 1995,
530 Soulsby et al. 2004, Blumstock et al. 2015). Soil depth, hydraulic conductivity, and baseflow index were
531 correspondingly high in streams from Clusters 1 and 4 that overlay the lower portion of the watershed (Figure 6).
532 Thermal sensitivities reflected this pattern, wherein generally sites draining low elevation tributaries (Cluster 1) had
533 relatively constant thermal sensitivities throughout the year (Figure 4). Conversely, the upper portion of the
534 Snoqualmie basin is covered by thin soil over impermeable bedrock lacking extensive fracture networks, meaning that
535 rain and snowmelt are not retained in the mountains but are rapidly transmitted to the stream system (Debose and
536 Klungland 1964, Nelson 1971, Goldin 1973, 1992). Sites with catchments predominantly within this upland area
537 tended to belong to Clusters 2 and 3 and displayed high summer thermal sensitivities, perhaps indicating limited
538 groundwater influence.

539 In the Wenatchee basin, two major aquifers exist: an aquifer within the sedimentary bedrock of the central
540 and lowland areas and an overlying unconsolidated alluvial and outwash aquifer located primarily in river valley
541 bottoms across the basin (Montgomery Water Group 2003). The bedrock aquifer consists of sandstones and shales,
542 which tend to have moderately low permeability. Folding and faulting have caused the shale to break up or fracture
543 and groundwater moves preferentially within these zones of higher secondary permeability. The alluvial and outwash
544 aquifers, on the other hand, exhibit relatively high permeability where groundwater can move easily and are considered

546 the primary groundwater source (Wildrick 1979, Montgomery Water Group 2003). Cluster 2 in the Wenatchee basin,
547 consisting of a single site located at the mouth of Chumstick Creek (Figure S5), stands out for having a unique, nearly
548 flat thermal sensitivity compared to patterns at other sites (Figure 5). Covariate distributions for the clustering results
549 showed that Chumstick Creek has a relatively high hydraulic conductivity and baseflow index (Figure 6; Figure S8).
550 A transition from low to high permeability glacial material occurs near the mouth of Chumstick Creek (Montgomery
551 Water Group 2003), and it is possible that substantial groundwater discharge occurs near this discontinuity (Neff et
552 al. 2019). Similarly, sites within Cluster 3 showed low variability in thermal sensitivity and had high soil depth and
553 baseflow index values. Streams within this cluster are situated on top of predominantly sandstone bedrock (Frizzell
554 1979, Gendaszek et al. 2014).

555 Overall, the importance of groundwater is consistent with previous studies, which find that thermal sensitivity
556 decreased with increasing groundwater contribution (O'Driscoll and DeWalle 2006, Chang and Pсарis 2013, Beaufort
557 et al. 2020, Georges et al. 2021). The degree to which groundwater decouples trends in stream and air temperature
558 depends on stream volume, the rate of groundwater inflow, and the depth of groundwater source. Although not
559 examined in this study, aquifer source and groundwater depth likely influence thermal sensitivity estimates, with
560 runoff sourced from deep groundwater being less variable and less sensitive in comparison to groundwater sourced
561 from shallow sub-surface flows (Tague et al. 2007, Johnson et al. 2021, Hare et al. 2021). Shallow groundwater
562 temperatures are already responding to climate change (Menberg et al. 2014). As warming continues, the summer
563 cooling capacity of groundwater may be reduced, limiting the availability of cold-water refugia patches sourced by
564 groundwater (Brewer 2013, Briggs et al. 2013).

565 **4.4 Landscape controls on thermal sensitivity**

566 Variable relationships between thermal sensitivities and landscape covariates highlight complexities in stream thermal
567 regimes. For example, mean channel slope was an important predictor of cluster membership for both the Snoqualmie
568 and Wenatchee basins, but showed a weak-to-non-existent relationship with summer thermal sensitivity summary
569 metrics. Steeper channel slopes and greater stream velocities limit warming in streams by decreasing the time for
570 equilibration with local heating conditions (Donato 2002, Webb et al. 2008, Isaak et al. 2012) and topographic shading
571 associated with steep watersheds can suppresses stream temperature by reducing exposure to solar radiation (Webb
572 and Zhang 1997). In the Wenatchee basin, the Cluster 3 site, Chumstick Creek, drains a steep canyon. This may
573 contribute to observed low, stable thermal sensitivities throughout the year. Additionally, watershed size and distance

Deleted: 7

575 upstream covary closely and displayed relatively consistent relationships with summer thermal sensitivity summary
576 metrics despite ranking moderately in variable importance. We expected thermal sensitivity to increase with river size;
577 groundwater influence should be more visible on smaller streams because the volume of water is small and the travel
578 time of the water from the source is short and not sufficient to equilibrate water temperature with the atmosphere
579 (Mohseni and Stefan 1999, Tague et al. 2007, Beaufort et al. 2016). Reduced sensitivity of headwater streams to air
580 temperature was observed in the Aberdeenshire Dee, Scotland (Hrachowitz et al. 2010), and River Danube, Austria
581 (Webb and Nobilis 2007), and small Pennsylvanian streams were shown to be less sensitive to changes in air
582 temperature than larger streams (Kelleher et al. 2012). However, Hilderbrand et al. (2014) found no relationship
583 between thermal sensitivity and watershed size in Maryland streams.

584 We expected landscape covariates to be important predictors of thermal sensitivity regimes, however, these
585 covariates were of limited importance and showed no relationship with summary metrics (Table 1B; Figure 6). Several
586 factors may account for this. Inherent covariation in river basins can hinder statistical efforts to identify mechanistic
587 links between landscape gradients and features of aquatic ecosystems (Lucero et al. 2011); land cover characteristics
588 may have a small impact that went undetected due to noisy observations or limited variability within our study region.
589 It is also possible that land cover metrics may not adequately describe the intended process. For example, the relative
590 unimportance of riparian shading may be due in part to our metric of shade, which was limited to riparian forest cover
591 and ignored topographic shading and vegetation height. Lastly, human modifications to the river that are not captured
592 by land cover statistics, such as channelization or the presence of dams and reservoirs, may alter thermal sensitivity
593 and obscure natural gradients. For example, areas of the river that are degraded and subsequently disconnected from
594 their floodplain may have artificially high thermal sensitivities, and the release of water from dams and reservoirs has
595 the potential to either warm or cool downstream temperatures, depending on dynamics of where and how impounded
596 water is released (Ahmad et al. 2021, Cheng et al. 2022). Future research could include covariates sinuosity or variance
597 of thalweg depth to better capture these effects. Untangling exact controls will require additional research.

598 **4.5 Assessment of statistical approach**

599 Collecting data on dynamic stream networks over time has inherent challenges that lead to relatively low sample sizes
600 and missing data as well as complex correlation structures across space and time. Our statistical approach was
601 designed to manage these challenges, enabling exploration of several hypotheses. These data, collected at a relatively

Deleted: Table 3

Deleted: Caveats and limitations

Deleted:

605 large number of sites in a parallel structure across two basins allow an assessment of how sensitive the statistical
606 approach may be to these constraints.

607 The time series of both air and water temperature used in this analysis have periods of missing values that
608 span weeks to months. Classical clustering techniques require complete datasets, limiting analyses to time series
609 without gaps. To overcome this issue, we calculated a single representative time series at each site that captures the
610 typical range and timing of thermal sensitivity. Alternative options for dealing with missing values include removing
611 data points that do not cover the target time period or imputing missing values by means of statistical procedures or
612 summary metrics (e.g., Savoy et al. 2019, Beaufort et al. 2020). However, we chose not to use these approaches in our
613 study due to the long and inconsistent periods of missing values across sites. We acknowledge that interannual
614 variability in precipitation and temperature impacts river thermal sensitivity, and average time series calculated from
615 differing years may exhibit differences in shape and timing for reasons outside of inherent characteristics (Appendix
616 A). Future studies could use novel clustering methods capable of dealing with sparse datasets, which would provide
617 more detailed information on clusters generated from time periods with robust values versus data scarcity (Carro-
618 Calvo et al. 2021). Alternatively, recent advances in space-time imputation for river basins may prove a fruitful
619 direction (Li et al. 2017).

620 Our calculation of time-varying thermal sensitivities also necessitated decisions regarding what features of the
621 time series to preserve. Selection of the bandwidth parameter and kernel function for the time varying model will
622 impact estimation of thermal sensitivity and intercept. Generally, with larger bandwidth estimates or averaging periods
623 (e.g., daily, weekly, monthly), intercept estimates increase and thermal sensitivity estimates decrease. Decisions of
624 this nature should be approached carefully and with a clear question in mind. For this study, we were interested in
625 seasonal to annual patterns in thermal sensitivity, and thus chose a bandwidth of 0.2, resulting in a smooth seasonal
626 time series. Previous studies have also used regression splines to estimate the time varying relationship between air
627 and water temperatures (Haggarty et al. 2015). This approach smooths data and can account for missing data but may
628 not preserve small-scale features of interest. We chose to use absolute values of our thermal sensitivity time series, as
629 we cared about differences in mean thermal sensitivity as well as correlated variability. Future work could normalize
630 thermal sensitivity time series first to examine only patterns.

631 While general patterns could be detected through our analysis, the details were sensitive to exactly which
632 sites were sampled and included in the analysis (Figure S7). In dynamic river systems with high spatial heterogeneity

Deleted: Due to the realities of data collection in dynamic systems,...

Formatted: Indent: First line: 0.5"

Deleted:

636 and inherent difficulties with accessing certain areas of the network, this is always likely to be true. Our approach of
637 averaging across years and clustering across sites appears to manage these realities well and provide general guidance
638 on the river networks sampled. For example, cross validation results for CART modelling suggest that certain
639 variables were consistently identified as more influential for cluster prediction and that results were relatively robust
640 to the inclusion of individual data points (Figure S7). Strengthening the assessment of underlying drivers and controls
641 to provide guidance for unsampled river networks will require that similar data sets are collected across more and
642 more river networks. Data can then be assembled and analysed to provide more general conclusions about geologic,
643 and climatic controls of river thermal regimes.

Deleted: geologic

644 **4.6 Implications for management and future directions**

645 Classifying rivers based on thermal sensitivity could be a powerful tool when planning for global change. Our results
646 show that annual patterns in thermal sensitivity are diverse and mediated by underlying geology and climate across
647 two Pacific Northwest river basins. Climate change is decreasing snowpack in the region, resulting in earlier runoff
648 and extended summer baseflow (Elsner et al. 2010, Wu et al. 2012), and may decrease groundwater discharge
649 depending on sources and timing of recharge (Brooks et al. 2012, McGill et al. 2021). For many of our study sites,
650 thermal sensitivities were highest in late summer during the hottest, lowest flow portion of the year. Previous studies
651 have found that the impact of fluctuations in discharge generally increases during dry, warm periods, when rivers have
652 a lower thermal capacity and are more sensitive to atmospheric warming (van Vliet et al. 2013). High thermal
653 sensitivity in late summer and in high elevation streams, which are typically thought to be climate refuges, is therefore
654 troubling for the conservation of native coldwater species such as Pacific salmon (Mantua et al. 2010; Isaak et al.
655 2016). Climate change will likely decrease juvenile rearing and spawning habitat quantity and quality, although it is
656 important to note that streams with high thermal sensitivity may still provide adequate habitat in select portions of the
657 year if stress-related thresholds are not exceeded (Armstrong et al. 2021).

658 Examining thermal sensitivity regimes improves understanding of factors contributing to stream
659 temperatures and may enable managers to target mitigation and adaptation activities to work best with local conditions,
660 thus maximizing benefits given limited resources. For example, given the importance of subsurface geology within
661 the Wenatchee and Snoqualmie basins, targeted actions to restore floodplain functions that recharge aquifers through
662 actions such as placing engineered logjams or reintroducing beavers could be prioritized (Abbe and Brooks 2013,
663 Pollock et al. 2014, Jordan and Fairfax 2022). Additionally, identification of particularly insensitive portions of the

665 river could help to better constrain areas where coldwater patches exist that may be used as refuges for coldwater fish
666 (Snyder et al. 2020). This process-based approach will be particularly important as non-stationary relationships caused
667 by climate change make it unreliable to use past regressions built under historical climate conditions (Boyer et al.
668 2021). Furthermore, as longer, more spatially extensive air and water temperature time series become available (Isaak
669 et al. 2017), we can begin to ask questions about 1) the spatial extent of different thermal sensitivity regimes, 2) how
670 interannual variability shifts with climate conditions and geographic context, and 3) detect changes in the external
671 drivers of thermal sensitivities. Such insights will improve our understanding of river ecosystems while offering a
672 suite of new tools for monitoring the impact of management decisions and climate change.

673 **Acknowledgements**

674 We thank Amy Marsha, Roxana Rautu, Akida Ferguson, Shannon Claeson and the many volunteers for help collecting
675 air and water temperature data, and Gordon Holtgrieve, Mark Scheuerell, and Christopher Jordan for suggestions that
676 improved the manuscript. This material is based upon work supported by the National Science Foundation Graduate
677 Research Fellowship under Grant No. DGE-1762114. Any opinion, findings, and conclusions or recommendations
678 expressed in this material are those of the authors and do not necessarily reflect the views of the National Science
679 Foundation.

680 **Author Contributions and Data Availability**

681 All authors conceptualized the study and retrieved the data. LMM analyzed the data and prepared the manuscript with
682 the assistance of EAS and AHF. The data that supports the findings of this study are available at
683 <https://github.com/lmcgill/AirWaterCorr/tree/master/data> and can be visualized at
684 https://lmcgill.shinyapps.io/TimeVarying_AWC/. The authors have no competing interests to declare.

685 **References**

- 686 Abbe, T., and A. Brooks. 2013. Geomorphic, Engineering, and Ecological Considerations when Using Wood in River
687 Restoration. Pages 419–451 in A. Simon, S. J. Bennett, and J. M. Castro, editors. Geophysical Monograph
688 Series. American Geophysical Union, Washington, D. C.
- 689 Ahmad, S. K., F. Hossain, G. W. Holtgrieve, T. Pavelsky, and S. Galelli. 2021. Predicting the Likely Thermal Impact
690 of Current and Future Dams Around the World. *Earth's Future* 9.
- 691 Arbelaitz, O., I. Gurrutxaga, J. Muguerza, J. M. Pérez, and I. Perona. 2013. An extensive comparative study of cluster
692 validity indices. *Pattern Recognition* 46:243–256.
- 693 Arismendi, I., M. Safeeq, J. B. Dunham, and S. L. Johnson. 2014. Can air temperature be used to project influences
694 of climate change on stream temperature? *Environmental Research Letters* 9:084015.
- 695 Armstrong, J. B., A. H. Fullerton, C. E. Jordan, J. L. Ebersole, J. R. Bellmore, I. Arismendi, B. E. Penaluna, and G.
696 H. Reeves. 2021. The importance of warm habitat to the growth regime of cold-water fishes. *Nature Climate
697 Change* 11:354–361.
- 698 Barnett, T. P., J. C. Adam, and D. P. Lettenmaier. 2005. Potential impacts of a warming climate on water availability
699 in snow-dominated regions. *Nature* 438:303–309.
- 700 Beaufort, A., F. Moatar, F. Curie, A. Ducharne, V. Bustillo, and D. Thiéry. 2016. River Temperature Modelling by
701 Strahler Order at the Regional Scale in the Loire River Basin, France: River Temperature Modelling by
702 Strahler Order. *River Research and Applications* 32:597–609.
- 703 Beaufort, A., F. Moatar, E. Sauquet, P. Loicq, and D. M. Hannah. 2020. Influence of landscape and hydrological
704 factors on stream–air temperature relationships at regional scale. *Hydrological Processes* 34:583–597.
- 705 Benyahya, L., D. Caissie, N. El-Jabi, and M. G. Satish. 2010. Comparison of microclimate vs. remote meteorological
706 data and results applied to a water temperature model (Miramichi River, Canada). *Journal of Hydrology*
707 380:247–259.
- 708 Bethel, J. 2004. An overview of the geology and geomorphology of the Snoqualmie River watershed. King County
709 Water and Land Resources Division, Snoqualmie Watershed Team.
- 710 Blumstock, M., D. Tetzlaff, I. A. Malcolm, G. Nuetzmann, and C. Soulsby. 2015. Baseflow dynamics: Multi-tracer
711 surveys to assess variable groundwater contributions to montane streams under low flows. *Journal of
712 Hydrology* 527:1021–1033.

713 Bogan, T., O. Mohseni, and H. G. Stefan. 2003. Stream temperature-equilibrium temperature relationship. *Water*
714 *Resources Research* 39.

715 Bower, D., D. M. Hannah, and G. R. McGregor. 2004. Techniques for assessing the climatic sensitivity of river flow
716 regimes. *Hydrological Processes* 18:2515–2543.

717 Boyer, C., A. St-Hilaire, and N. E. Bergeron. 2021. Defining river thermal sensitivity as a function of climate. *River*
718 *Research and Applications* 37:1548–1561.

719 Breiman, L., J. H. Friedman, R. A. Olshen, and C. J. Stone. 1984. *Classification And Regression Trees*. First edition.
720 Routledge.

721 Brennan, S. R., D. E. Schindler, T. J. Cline, T. E. Walsworth, G. Buck, and D. P. Fernandez. 2019. Shifting habitat
722 mosaics and fish production across river basins. *Science* 364:783–786.

723 Brewer, S. K. 2013. GROUNDWATER INFLUENCES ON THE DISTRIBUTION AND ABUNDANCE OF
724 RIVERINE SMALLMOUTH BASS, *MICROPTERUS DOLOMIEU*, IN PASTURE LANDSCAPES OF
725 THE MIDWESTERN USA. *River Research and Applications* 29:269–278.

726 Briggs, M. A., P. Goodling, Z. C. Johnson, K. M. Rogers, N. P. Hitt, J. B. Fair, and C. D. Snyder. 2022. Bedrock depth
727 influences spatial patterns of summer baseflow, temperature, and flow disconnection for mountainous
728 headwater streams. preprint, *Catchment hydrology/Instruments and observation techniques*.

729 Briggs, M. A., Z. C. Johnson, C. D. Snyder, N. P. Hitt, B. L. Kurylyk, L. Lautz, D. J. Irvine, S. T. Hurley, and J. W.
730 Lane. 2018. Inferring watershed hydraulics and cold-water habitat persistence using multi-year air and stream
731 temperature signals. *Science of The Total Environment* 636:1117–1127.

732 Briggs, M. A., E. B. Voytek, F. D. Day-Lewis, D. O. Rosenberry, and J. W. Lane. 2013. Understanding Water Column
733 and Streambed Thermal Refugia for Endangered Mussels in the Delaware River. *Environmental Science &*
734 *Technology* 47:11423–11431.

735 Brooks, J. R., P. J. Wigington, D. L. Phillips, R. Comeleo, and R. Coulombe. 2012. Willamette River Basin surface
736 water isoscape ($\delta^{18}\text{O}$ and $\delta^2\text{H}$): temporal changes of source water within the river. *Ecosphere* 3:art39.

737 Cadbury, S. L., D. M. Hannah, A. M. Milner, C. P. Pearson, and L. E. Brown. 2008. Stream temperature dynamics
738 within a New Zealand glacierized river basin. *River Research and Applications* 24:68–89.

739 Carro-Calvo, L., F. Jaume-Santero, R. García-Herrera, and S. Salcedo-Sanz. 2021. k-Gaps: a novel technique for
740 clustering incomplete climatological time series. *Theoretical and Applied Climatology* 143:447–460.

741 Casas, I., and R. Fernandez-Casal. 2019. tvReg: Time-varying Coefficient Linear Regression for Single and Multi-
742 Equations in R. SSRN Electronic Journal.

743 Casas, I., and R. Fernandez-Casal. 2021. tvReg: Time-Varying Coefficients Linear Regression for Single and Multi-
744 Equations.

745 Chang, H., and M. Pсарis. 2013. Local landscape predictors of maximum stream temperature and thermal sensitivity
746 in the Columbia River Basin, USA. *Science of The Total Environment* 461–462:587–600.

747 Charrad, M., N. Ghazzali, V. Boiteau, and A. Niknafs. 2014. NbClust: An R Package for Determining the Relevant
748 Number of Clusters in a Data Set. *Journal of Statistical Software* 61:1–36.

749 Cheng, Y., B. Nijssen, G. W. Holtgrieve, and J. D. Olden. 2022. Modeling the freshwater ecological response to
750 changes in flow and thermal regimes influenced by reservoir dynamics. *Journal of Hydrology* 608:127591.

751 Chu, C., N. E. Jones, and L. Allin. 2010. Linking the thermal regimes of streams in the Great Lakes Basin, Ontario,
752 to landscape and climate variables: THERMAL REGIMES IN ONTARIO STREAMS. *River Research and*
753 *Applications* 26:221–241.

754 Cline, T. J., D. E. Schindler, T. E. Walsworth, D. W. French, and P. J. Lisi. 2020. Low snowpack reduces thermal
755 response diversity among streams across a landscape. *Limnology and Oceanography Letters* 5:254–263.

756 Cressie, N. A. C. 1993. *Statistics for Spatial Data: Cressie/Statistics*. John Wiley & Sons, Inc., Hoboken, NJ, USA.

757 Daufresne, M., and P. Boët. 2007. Climate change impacts on structure and diversity of fish communities in rivers.
758 *Global Change Biology* 13:2467–2478.

759 De'ath, G., and K. E. Fabricius. 2000. Classification and regression trees: a powerful yet simple technique for
760 ecological data analysis. *Ecology* 81:3178–3192.

761 Debose, A., and M. W. Klungland. 1964. Soil survey of Snohomish County area. US Department of Agriculture, Soil
762 Conservation Service, Washington, D. C.

763 Donato, M. M. 2002. A statistical model for estimating stream temperatures in the Salmon and Clearwater River
764 basins, Central Idaho. Water Resources Investigations Report, U.S. Geological Survey, Washington, D. C.

765 Elsner, M. M., L. Cuo, N. Voisin, J. S. Deems, A. F. Hamlet, J. A. Vano, K. E. B. Mickelson, S.-Y. Lee, and D. P.
766 Lettenmaier. 2010. Implications of 21st century climate change for the hydrology of Washington State.
767 *Climatic Change* 102:225–260.

768 Frizzell, V. A. 1979. Petrology and stratigraphy of Paleogene nonmarine sandstones, Cascade Range, Washington.
769 Open-File Report, U.S. Geological Survey.

770 Garner, G., D. M. Hannah, J. P. Sadler, and H. G. Orr. 2014. River temperature regimes of England and Wales: spatial
771 patterns, inter-annual variability and climatic sensitivity: RIVER TEMPERATURE REGIMES OF
772 ENGLAND AND WALES. *Hydrological Processes* 28:5583–5598.

773 Gendaszek, A. S., D. M. Ely, S. R. Hinkle, S. C. Kahle, and W. B. Welch. 2014. Hydrogeologic framework and
774 groundwater/surface-water interactions of the upper Yakima River Basin, Kittitas County, central
775 Washington. Scientific Investigations Report, U.S. Geological Survey.

776 Georges, B., A. Michez, H. Piegay, L. Huylenbroeck, P. Lejeune, and Y. Brostaux. 2021. Which environmental factors
777 control extreme thermal events in rivers? A multi-scale approach (Wallonia, Belgium). *PeerJ* 9:e12494.

778 Goldin, A. 1973. Soil survey of King County area, Washington. US Department of Agriculture, Soil Conservation
779 Service, Washington, D. C.

780 Goldin, A. 1992. Soil survey of Whatcom County area, Washington. US Department of Agriculture, Soil Conservation
781 Service, Washington, D. C.

782 Haggarty, R. A., C. A. Miller, and E. M. Scott. 2015. Spatially weighted functional clustering of river network data.
783 *Journal of the Royal Statistical Society: Series C (Applied Statistics)* 64:491–506.

784 Hare, D. K., A. M. Helton, Z. C. Johnson, J. W. Lane, and M. A. Briggs. 2021. Continental-scale analysis of shallow
785 and deep groundwater contributions to streams. *Nature Communications* 12:1450.

786 Hennig, C. 2020. *fpc: Flexible Procedures for Clustering*.

787 Hilderbrand, R. H., M. T. Kashiwagi, and A. P. Prochaska. 2014. Regional and Local Scale Modeling of Stream
788 Temperatures and Spatio-Temporal Variation in Thermal Sensitivities. *Environmental Management* 54:14–
789 22.

790 Hill, R. A., M. H. Weber, S. G. Leibowitz, A. R. Olsen, and D. J. Thornbrugh. 2016. The Stream-Catchment
791 (StreamCat) Dataset: A Database of Watershed Metrics for the Conterminous United States. *JAWRA Journal*
792 *of the American Water Resources Association* 52:120–128.

793 Hoover, D. 1998. Nonparametric smoothing estimates of time-varying coefficient models with longitudinal data.
794 *Biometrika* 85:809–822.

795 Hrachowitz, M., C. Soulsby, C. Imholt, I. A. Malcolm, and D. Tetzlaff. 2010. Thermal regimes in a large upland
796 salmon river: a simple model to identify the influence of landscape controls and climate change on maximum
797 temperatures. *Hydrological Processes* 24:3374–3391.

798 Isaak, D. J., C. H. Luce, G. L. Chandler, D. L. Horan, and S. P. Wollrab. 2018a. Principal components of thermal
799 regimes in mountain river networks. *Hydrology and Earth System Sciences* 22:6225–6240.

800 Isaak, D. J., C. H. Luce, D. L. Horan, G. L. Chandler, S. P. Wollrab, W. B. Dubois, and D. E. Nagel. 2020. Thermal
801 Regimes of Perennial Rivers and Streams in the Western United States. *JAWRA Journal of the American*
802 *Water Resources Association* 56:842–867.

803 Isaak, D. J., C. H. Luce, D. L. Horan, G. L. Chandler, S. P. Wollrab, and D. E. Nagel. 2018b. Global Warming of
804 Salmon and Trout Rivers in the Northwestern U.S.: Road to Ruin or Path Through Purgatory? *Transactions*
805 *of the American Fisheries Society* 147:566–587.

806 Isaak, D. J., S. J. Wenger, E. E. Peterson, J. M. Ver Hoef, D. E. Nagel, C. H. Luce, S. W. Hostetler, J. B. Dunham, B.
807 B. Roper, S. P. Wollrab, G. L. Chandler, D. L. Horan, and S. Parkes-Payne. 2017. The NorWeST Summer
808 Stream Temperature Model and Scenarios for the Western U.S.: A Crowd-Sourced Database and New
809 Geospatial Tools Foster a User Community and Predict Broad Climate Warming of Rivers and Streams.
810 *Water Resources Research* 53:9181–9205.

811 Isaak, D. J., S. Wollrab, D. Horan, and G. Chandler. 2012. Climate change effects on stream and river temperatures
812 across the northwest U.S. from 1980–2009 and implications for salmonid fishes. *Climatic Change* 113:499–
813 524.

814 Isaak, D. J., M. K. Young, C. H. Luce, S. W. Hostetler, S. J. Wenger, E. E. Peterson, J. M. Ver Hoef, M. C. Groce, D.
815 L. Horan, and D. E. Nagel. 2016. Slow climate velocities of mountain streams portend their role as refugia
816 for cold-water biodiversity. *Proceedings of the National Academy of Sciences* 113:4374–4379.

817 Jackson, F. L., R. J. Fryer, D. M. Hannah, C. P. Millar, and I. A. Malcolm. 2018. A spatio-temporal statistical model
818 of maximum daily river temperatures to inform the management of Scotland’s Atlantic salmon rivers under
819 climate change. *Science of The Total Environment* 612:1543–1558.

820 Johnson, S. L. 2003. Stream temperature: scaling of observations and issues for modelling. *Hydrological Processes*
821 17:497–499.

822 Johnson, Z. C., B. G. Johnson, M. A. Briggs, C. D. Snyder, N. P. Hitt, and W. D. Devine. 2021. Heed the data gap:
823 Guidelines for using incomplete datasets in annual stream temperature analyses. *Ecological Indicators*
824 122:107229.

825 Johnson, Z. C., C. D. Snyder, and N. P. Hitt. 2017. Landform features and seasonal precipitation predict shallow
826 groundwater influence on temperature in headwater streams. *Water Resources Research* 53:5788–5812.

827 Johnson, Z. C., J. J. Warwick, and R. Schumer. 2014. Factors affecting hyporheic and surface transient storage in a
828 western U.S. river. *Journal of Hydrology* 510:325–339.

829 Jordan, C. E., and E. Fairfax. 2022. Beaver: The North American freshwater climate action plan. *WIREs Water* 9.

830 Kelleher, C. A., H. E. Golden, and S. A. Archfield. 2021. Monthly river temperature trends across the US confound
831 annual changes. *Environmental Research Letters* 16:104006.

832 Kelleher, C., T. Wagener, M. Gooseff, B. McGlynn, K. McGuire, and L. Marshall. 2012. Investigating controls on the
833 thermal sensitivity of Pennsylvania streams. *Hydrological Processes* 26:771–785.

834 Krzywinski, M., and N. Altman. 2017. Classification and regression trees. *Nature Methods* 14:757–758.

835 Lance, G. N., and W. T. Williams. 1967. A general theory of classificatory sorting strategies: II. Clustering systems.
836 *The Computer Journal* 10:271–277.

837 Leach, J. A., C. Kelleher, B. L. Kurylyk, R. D. Moore, and B. T. Neilson. 2023. A primer on stream temperature
838 processes. *WIREs Water* 10:e1643.

839 Leach, J. A., and R. D. Moore. 2019. Empirical Stream Thermal Sensitivities May Underestimate Stream Temperature
840 Response to Climate Warming. *Water Resources Research* 55:5453–5467.

841 Li, H., X. Deng, C. A. Dolloff, and E. P. Smith. 2016. Bivariate functional data clustering: grouping streams based on
842 a varying coefficient model of the stream water and air temperature relationship. *Environmetrics* 27:15–26.

843 Li, H., X. Deng, D.-Y. Kim, and E. P. Smith. 2014. Modeling maximum daily temperature using a varying coefficient
844 regression model. *Water Resources Research* 50:3073–3087.

845 Li, H., X. Deng, and E. Smith. 2017. Missing data imputation for paired stream and air temperature sensor data:
846 Missing Data Imputation for Stream and Air Temperature. *Environmetrics* 28:e2426.

847 Lisi, P. J., D. E. Schindler, T. J. Cline, M. D. Scheuerell, and P. B. Walsh. 2015. Watershed geomorphology and
848 snowmelt control stream thermal sensitivity to air temperature. *Geophysical Research Letters* 42:3380–3388.

849 Luce, C., B. Staab, M. Kramer, S. Wenger, D. Isaak, and C. McConnell. 2014. Sensitivity of summer stream
850 temperatures to climate variability in the Pacific Northwest. *Water Resources Research* 50:3428–3443.

851 Maheu, A., N. L. Poff, and A. St-Hilaire. 2016. A Classification of Stream Water Temperature Regimes in the
852 Conterminous USA: Classification of Stream Temperature Regimes. *River Research and Applications*
853 32:896–906.

854 Mantua, N., I. Tohver, and A. Hamlet. 2010. Climate change impacts on streamflow extremes and summertime stream
855 temperature and their possible consequences for freshwater salmon habitat in Washington State. *Climatic*
856 *Change* 102:187–223.

857 Mauger, S., R. Shaftel, J. C. Leppi, and D. J. Rinella. 2017. Summer temperature regimes in southcentral Alaska
858 streams: watershed drivers of variation and potential implications for Pacific salmon. *Canadian Journal of*
859 *Fisheries and Aquatic Sciences* 74:702–715.

860 Mayer, T. D. 2012. Controls of summer stream temperature in the Pacific Northwest. *Journal of Hydrology* 475:323–
861 335.

862 McGill, L. M., J. R. Brooks, and E. A. Steel. 2021. Spatiotemporal dynamics of water sources in a mountain river
863 basin inferred through $\Delta^2\text{H}$ and $\Delta^{18}\text{O}$ of water. *Hydrological Processes* 35.

864 Meier, W., C. Bonjour, A. Wüest, and P. Reichert. 2003. Modeling the Effect of Water Diversion on the Temperature
865 of Mountain Streams. *Journal of Environmental Engineering* 129:755–764.

866 Menberg, K., P. Blum, B. L. Kurylyk, and P. Bayer. 2014. Observed groundwater temperature response to recent
867 climate change. *Hydrology and Earth System Sciences* 18:4453–4466.

868 Mohseni, O., T. R. Erickson, and H. G. Stefan. 1999. Sensitivity of stream temperatures in the United States to air
869 temperatures projected under a global warming scenario. *Water Resources Research* 35:3723–3733.

870 Mohseni, O., and H. G. Stefan. 1999. Stream temperature/air temperature relationship: a physical interpretation.
871 *Journal of Hydrology* 218:128–141.

872 Mohseni, O., H. G. Stefan, and J. G. Eaton. 2003. Global Warming and Potential Changes in Fish Habitat in U.S.
873 Streams. *Climatic Change* 59:389–409.

874 Mohseni, O., H. G. Stefan, and T. R. Erickson. 1998. A nonlinear regression model for weekly stream temperatures.
875 *Water Resources Research* 34:2685–2692.

876 Montgomery Water Group. 2003. Wenatchee River Basin Watershed Assessment.

877 Musselman, K. N., N. Addor, J. A. Vano, and N. P. Molotch. 2021. Winter melt trends portend widespread declines
878 in snow water resources. *Nature Climate Change* 11:418–424.

879 Neff, B. P., D. O. Rosenberry, S. G. Leibowitz, D. M. Mushet, H. E. Golden, M. C. Rains, J. R. Brooks, and C. R.
880 Lane. 2019. A Hydrologic Landscapes Perspective on Groundwater Connectivity of Depressional Wetlands.
881 *Water* 12:50.

882 Nelson, L. M. 1971. Sediment transport by streams in the Snohomish River basin, Washington: October 1967-
883 June 1969.

884 O’Driscoll, M. A., and D. R. DeWalle. 2006. Stream–air temperature relations to classify stream–ground water
885 interactions in a karst setting, central Pennsylvania, USA. *Journal of Hydrology* 329:140–153.

886 Olden, J. D., M. J. Kennard, and B. J. Pusey. 2012. A framework for hydrologic classification with a review of
887 methodologies and applications in ecohydrology: A FRAMEWORK FOR HYDROLOGIC
888 CLASSIFICATION. *Ecohydrology* 5:503–518.

889 Olden, J. D., J. J. Lawler, and N. L. Poff. 2008. Machine Learning Methods Without Tears: A Primer for Ecologists.
890 *The Quarterly Review of Biology* 83:171–193.

891 Parkinson, E. A., E. V. Lea, M. A. Nelitz, J. M. Knudson, and R. D. Moore. 2016. Identifying Temperature Thresholds
892 Associated with Fish Community Changes in British Columbia, Canada, to Support Identification of
893 Temperature Sensitive Streams: STREAM TEMPERATURE AND FISH COMMUNITIES. *River Research
894 and Applications* 32:330–347.

895 Patton, N. R., K. A. Lohse, S. E. Godsey, B. T. Crosby, and M. S. Seyfried. 2018. Predicting soil thickness on soil
896 mantled hillslopes. *Nature Communications* 9:3329.

897 Pollock, M. M., T. J. Beechie, J. M. Wheaton, C. E. Jordan, N. Bouwes, N. Weber, and C. Volk. 2014. Using Beaver
898 Dams to Restore Incised Stream Ecosystems. *BioScience* 64:279–290.

899 Pyne, M. I., and N. L. Poff. 2017. Vulnerability of stream community composition and function to projected thermal
900 warming and hydrologic change across ecoregions in the western United States. *Global Change Biology*
901 23:77–93.

902 R Core Team. 2020. R: A Language and Environment for Statistical Computing. R Foundation for Statistical
903 Computing, Vienna, Austria.

904 Savoy, P., A. P. Appling, J. B. Heffernan, E. G. Stets, J. S. Read, J. W. Harvey, and E. S. Bernhardt. 2019. Metabolic
905 rhythms in flowing waters: An approach for classifying river productivity regimes. *Limnology and*
906 *Oceanography* 64:1835–1851.

907 Siegel, J. E., A. H. Fullerton, and C. E. Jordan. 2022. Accounting for snowpack and time-varying lags in statistical
908 models of stream temperature. *Journal of Hydrology X* 17:100136.

909 Snyder, C. D., N. P. Hitt, and J. A. Young. 2015. Accounting for groundwater in stream fish thermal habitat responses
910 to climate change. *Ecological Applications* 25:1397–1419.

911 Snyder, M. N., N. H. Schumaker, J. B. Dunham, M. L. Keefer, P. Leinenbach, A. Brookes, J. Palmer, J. Wu, D.
912 Keenan, and J. L. Ebersole. 2020. Assessing contributions of cold-water refuges to reproductive migration
913 corridor conditions for adult salmon and steelhead trout in the Columbia River, USA. *Journal of*
914 *Ecohydraulics*:1–13.

915 Soulsby, C., P. J. Rodgers, J. Petry, D. M. Hannah, I. A. Malcolm, and S. M. Dunn. 2004. Using tracers to upscale
916 flow path understanding in mesoscale mountainous catchments: two examples from Scotland. *Journal of*
917 *Hydrology* 291:174–196.

918 Steel, E. A., T. J. Beechie, C. E. Torgersen, and A. H. Fullerton. 2017. Envisioning, Quantifying, and Managing
919 Thermal Regimes on River Networks. *BioScience* 67:506–522.

920 Steel, E. A., A. Marsha, A. H. Fullerton, J. D. Olden, N. K. Larkin, S.-Y. Lee, and A. Ferguson. 2019. Thermal
921 landscapes in a changing climate: biological implications of water temperature patterns in an extreme year.
922 *Canadian Journal of Fisheries and Aquatic Sciences* 76:1740–1756.

923 Tague, C., M. Farrell, G. Grant, S. Lewis, and S. Rey. 2007. Hydrogeologic controls on summer stream temperatures
924 in the McKenzie River basin, Oregon. *Hydrological Processes* 21:3288–3300.

925 Therneau, T., and B. Atkinson. 2019. rpart: Recursive Partitioning and Regression Trees.

926 Thornton, M.M., Shrestha, R., Wei, Y., Thornton, P.E., Kao, S., and Wilson, B.E. 2020. DaymetDaymet: Daily
927 Surface Weather Data on a 1-km Grid for North America, Version 4:0 MB.

928 Turney, G. L., S. C. Kahle, and N. P. Dion. 1995. Geohydrology and ground-water quality of east King County,
929 Washington. Water Resources Investigations Report, Prepared in cooperation with Seattle-King County
930 Department of Health Tacoma, Washington, Washington, D. C.

931 Ver Hoef, J. M., and E. E. Peterson. 2010. A Moving Average Approach for Spatial Statistical Models of Stream
932 Networks. *Journal of the American Statistical Association* 105:6–18.

933 van Vliet, M. T. H., W. H. P. Franssen, J. R. Yearsley, F. Ludwig, I. Haddeland, D. P. Lettenmaier, and P. Kabat.
934 2013. Global river discharge and water temperature under climate change. *Global Environmental Change*
935 23:450–464.

936 van Vliet, M. T. H., F. Ludwig, J. J. G. Zwolsman, G. P. Weedon, and P. Kabat. 2011. Global river temperatures and
937 sensitivity to atmospheric warming and changes in river flow: SENSITIVITY OF GLOBAL RIVER
938 TEMPERATURES. *Water Resources Research* 47.

939 Webb, B. W., D. M. Hannah, R. D. Moore, L. E. Brown, and F. Nobilis. 2008. Recent advances in stream and river
940 temperature research. *Hydrological Processes* 22:902–918.

941 Webb, B. W., and F. Nobilis. 2007. Long-term changes in river temperature and the influence of climatic and
942 hydrological factors. *Hydrological Sciences Journal* 52:74–85.

943 Webb, B. W., and Y. Zhang. 1997. SPATIAL AND SEASONAL VARIABILITY IN THE COMPONENTS OF THE
944 RIVER HEAT BUDGET. *Hydrological Processes* 11:79–101.

945 Wildrick, L. 1979. Ground Water Flow System of the Chumstick Drainage Basin. Page 5. Washington State
946 Department of Ecology, Olympia, WA.

947 Winfree, M. M., E. Hood, S. L. Stuefer, D. E. Schindler, T. J. Cline, C. D. Arp, and S. Pyare. 2018. Landcover and
948 geomorphology influence streamwater temperature sensitivity in salmon bearing watersheds in Southeast
949 Alaska. *Environmental Research Letters* 13:064034.

950 Wolock, D. M., T. C. Winter, and G. McMahon. 2004. Delineation and Evaluation of Hydrologic-Landscape Regions
951 in the United States Using Geographic Information System Tools and Multivariate Statistical Analyses.
952 *Environmental Management* 34:S71–S88.

953 Wu, H., J. S. Kimball, M. M. Elsner, N. Mantua, R. F. Adler, and J. Stanford. 2012. Projected climate change impacts
954 on the hydrology and temperature of Pacific Northwest rivers: CLIMATE CHANGE IMPACTS ON
955 STREAMFLOW AND TEMPERATURE. *Water Resources Research* 48.

956 Yan, H., N. Sun, A. Fullerton, and M. Baerwalde. 2021. Greater vulnerability of snowmelt-fed river thermal regimes
957 to a warming climate. *Environmental Research Letters* 16:054006.

958

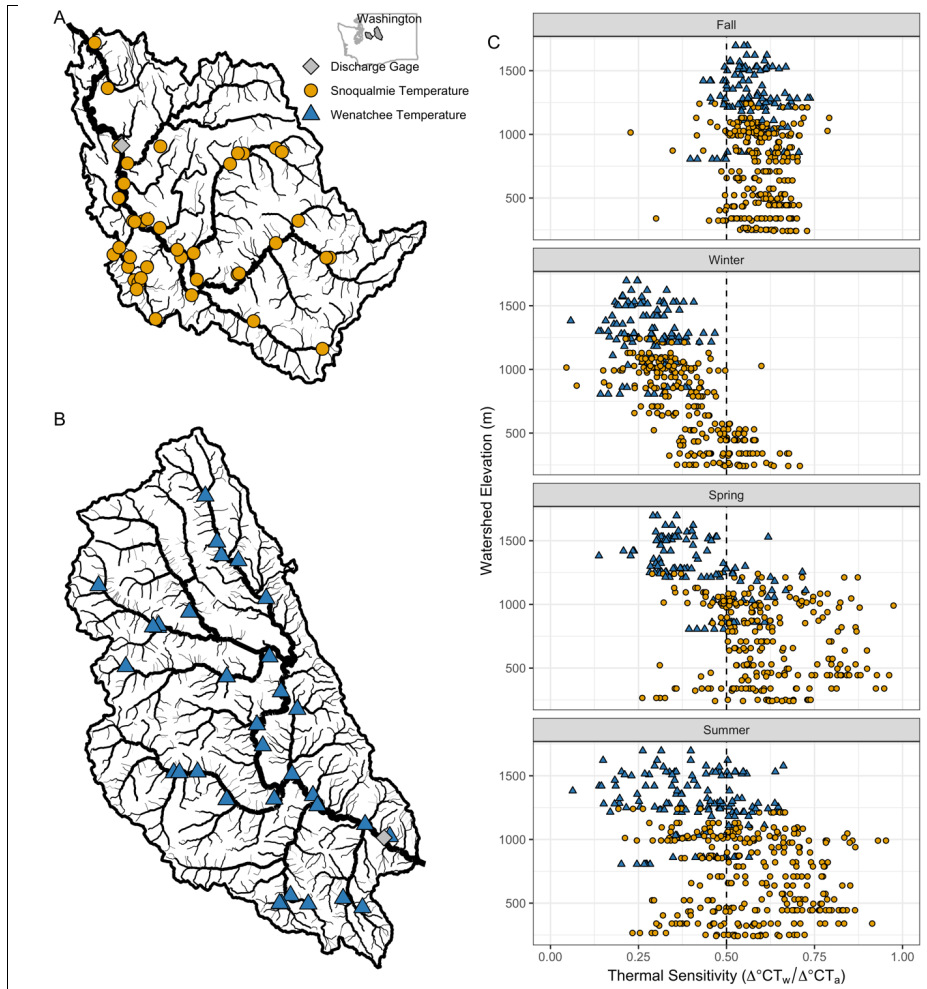


Figure 1. A map of the Snoqualmie (A) and Wenatchee (B) basins water and air temperature monitoring sites and the most downstream USGS gage for each basin. Thermal sensitivity, defined as the change in water temperature with a single degree change in air temperature, versus MWE for each site-year combination (C). *The dashed line in Figure 1C is included as a reference.*

959

960

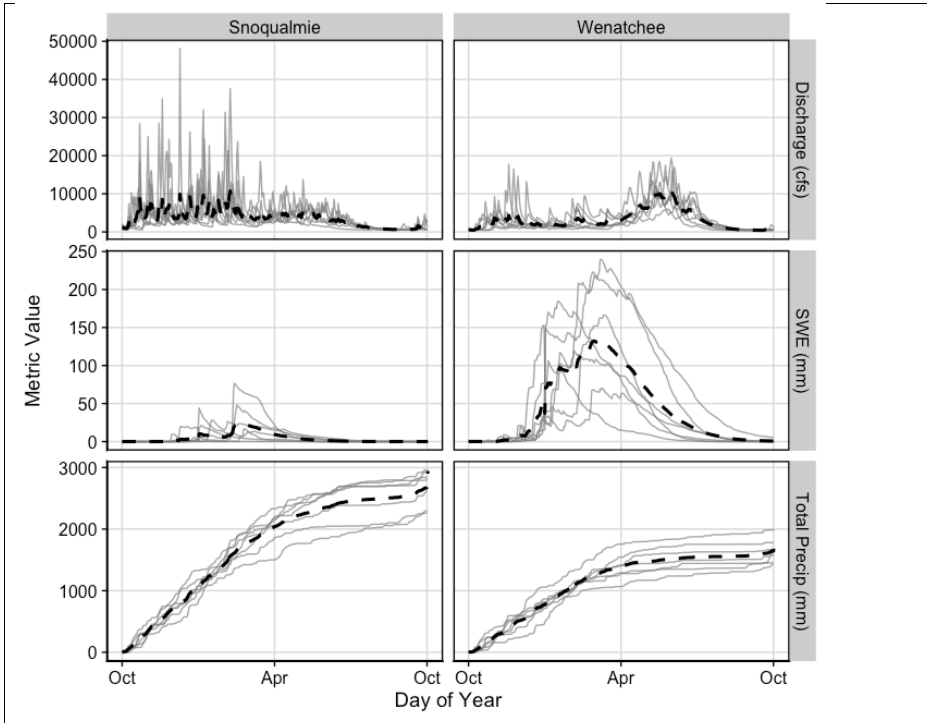


Figure 2. Average annual discharge, SWE, and total precipitation for the [outlets of the](#) Snoqualmie and Wenatchee basins across the sampling timeframe (black dashed lines) and interannual variability across the seven water years included in this analysis (gray lines). [Discharge gage locations can be found in Figure 1A and 1B, and SWE and precipitation data is from DAYMET Daily Surface Weather data for the upstream watershed of each discharge gage \(Thornton et al. 2020\).](#)

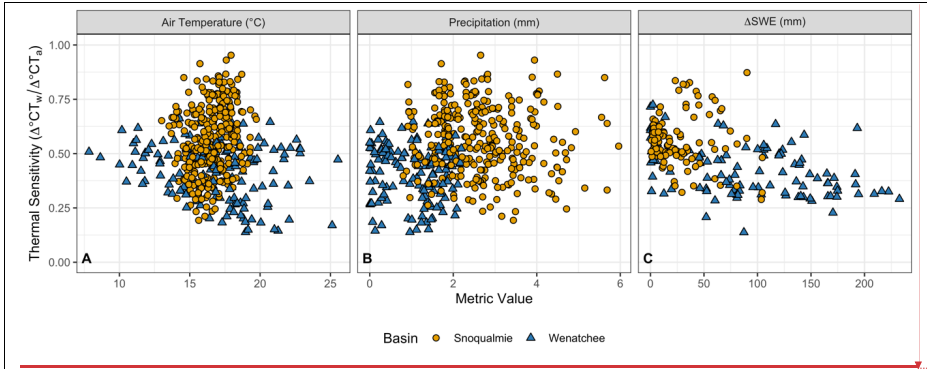
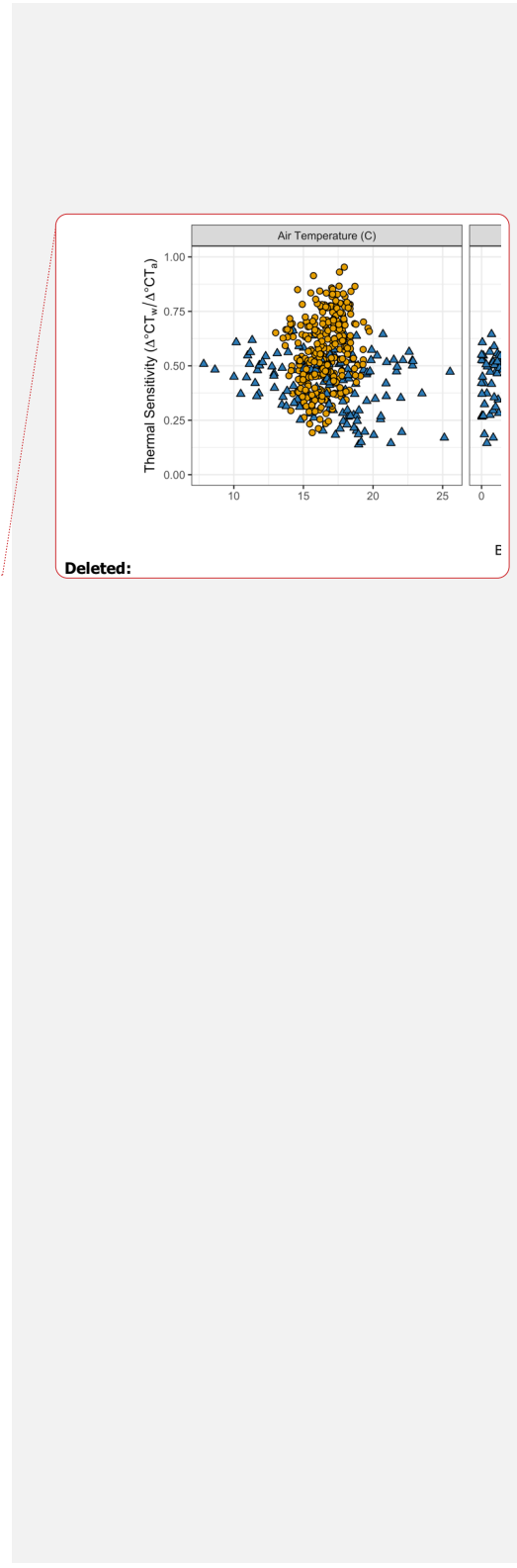


Figure 3. Summer thermal sensitivity values for all site-year combinations in the Snoqualmie and Wenatchee basins versus air temperature (A), and precipitation (B). Spring thermal sensitivity values for all site-year combinations versus total SWE (C) from gridded DAYMET data for each sampling point. Points are colored by basin. Basins that have no snowmelt in a given year are not shown on graph (C).



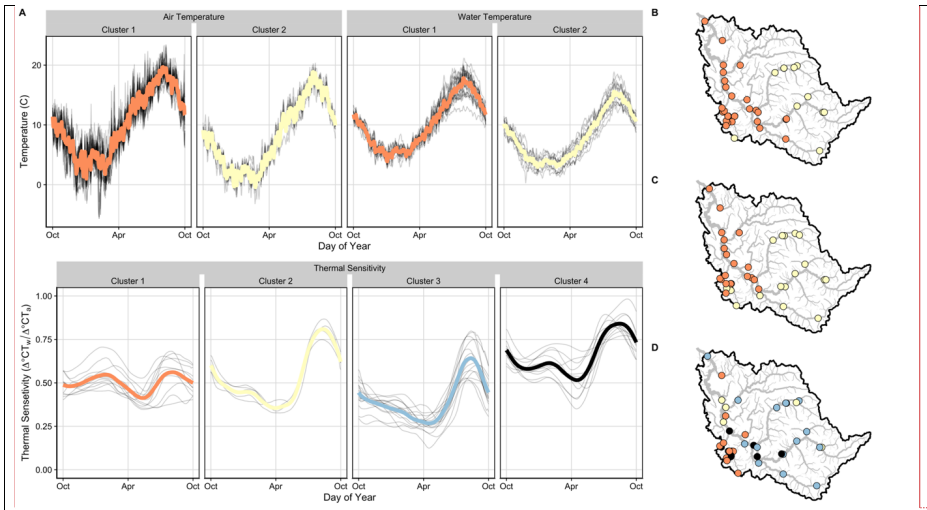


Figure 4. Average time series (A) and spatial clustering results (columns/colors indicate unique clusters) for average annual air temperature (B), water temperature (C), and thermal sensitivity (D) in the Snoqualmie basin. The spatial distribution for colored lines indicates mean average annual values for each cluster, and gray lines denote average annual values for each site within a given cluster.

Commented [LM7]: Add numbers to facet labels.

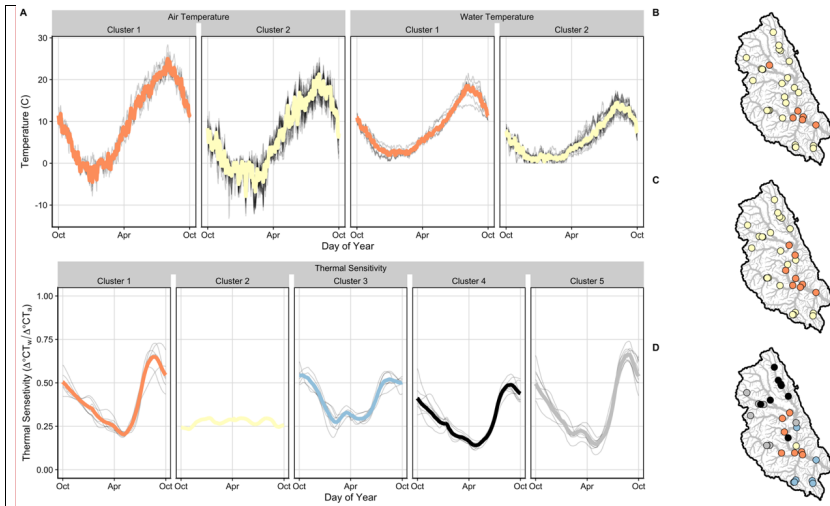


Figure 5. Average time series (A) and spatial clustering results (columns/colors indicate unique clusters) for average annual air temperature (B), water temperature (C), and thermal sensitivity (D) in the Wenatchee basin. The spatial distribution for colored lines indicates mean average annual values for each cluster, and gray lines denote average annual values for each site within a given cluster.

Commented [LM8]: Add numbers of facet labels.

Deleted:

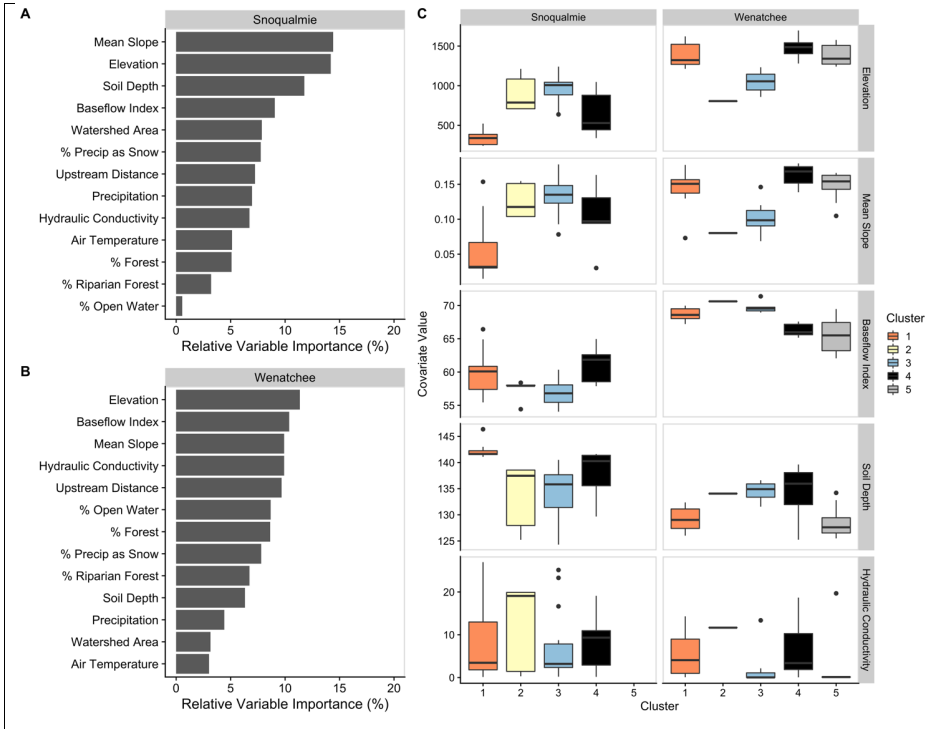


Figure 6. Relative variable importance for all covariates in the Snoqualmie (A) and Wenatchee (B) basins, and the distributions of variables across clusters for the four most important variables (C) in the Snoqualmie basin (Mean Slope, Elevation, Soil Depth, and Baseflow Index) and in the Wenatchee basin (Elevation, Baseflow Index, Mean Slope, and Hydraulic Conductivity). Boxes are grouped and colored by cluster membership. See Figure S8 for plots of the remaining relative variable importances.

Commented [HC9]: ? not sure if needed but a complex graph so worth detailing how to interpret

Deleted: 7

Deleted: s.

5 **Table 1.** Hypothesized relationships between landscape covariates and thermal sensitivity based on previous literature (A) and the observed relationship between landscape variables and thermal sensitivities within our study basins in summer (B). Loess curves are shown to aid in visualization and correlation coefficients quantify the strength of the linear relationship. See Figure S6 for a detailed description of how river attributes covary with one another.

Deleted: **Table 1.** Physical environmental data and basin characteristics used to predict air-water clusters.
 Variable ... [1]
Formatted: Tab stops: 0.95", Left
Deleted:Page Break.....
Table 3

| A. Hypothesized Drivers | | | B. Observed Relationship |
|---|--|--|--|
| Stream or watershed attribute (covarying variables) | Theoretical relationship with thermal sensitivity | Explanation | Observed Relationship in Summer |
| <u>Mean watershed slope</u> +elevation +dist upstream - soil depth | Negative | <ul style="list-style-type: none"> Increased snowmelt and cooling due to faster velocity water movement and shorter water residence time (Winfree et al. 2018). Topographic shading associated with steep watersheds suppresses stream temperature by reducing exposure to solar radiation (Webb and Zhang 1997). | |
| <u>Mean watershed elevation</u> +slope +dist upstream +% lake area - soil depth | Negative | <ul style="list-style-type: none"> Higher elevations have higher snowmelt accumulation and greater proportion of snowmelt in spring. The impact of elevation on spring and early summer stream temperature is diminished in years with low winter snow accumulation. | |
| <u>Distance upstream</u> - watershed size +slope +elevation | Negative | <ul style="list-style-type: none"> Duration of surface water's exposure to solar radiation and atmospheric energy flux is higher in low gradient watersheds with slower streamflow velocities (Poole and Berman 2001). | |
| <u>Percent riparian forest cover</u> +% forest cover - watershed size | Negative | <ul style="list-style-type: none"> Riparian vegetation provides shading to streams, reducing exposure to solar radiation (Webb and Zhang 1997), particularly during summer base flows. Forest canopy can influence snow accumulation within a watershed and snowmelt contribution to streams. Low density forests accumulate more snow relative to | |

| | | | |
|---|-----------------|---|--|
| | | <p>high density forests (Varhola et al 2010).</p> <ul style="list-style-type: none"> • Conversion of forested land area can accelerate runoff and reduce infiltration, warming surface flows before they reach stream channels (Naiman et al. 2005; Nelson and Palmer 2007). | |
| <p>Hydraulic Conductivity +baseflow index</p> | <p>Positive</p> | <ul style="list-style-type: none"> • Hydraulic conductivity refers to the ability of a geologic material to transmit water and is calculated from mean lithological hydraulic conductivity content in surface or near surface geology. • Relatively high hydraulic conductivity material would be represented by something like unconsolidated alluvial sands and gravels. • High hydraulic conductivity is typically associated with areas of greater groundwater activity and lower, more stable thermal sensitivity values. | |

Deleted: A. Hypothesized Drivers [21]

Table 2. Physical environmental data and basin characteristics used to predict air-water clusters.

| <u>Variable</u> | <u>Category</u> | <u>Units</u> | <u>Data Source</u> |
|---------------------------------|-------------------------|------------------------|---|
| <u>Watershed area</u> | <u>Basin Topography</u> | <u>km²</u> | <u>Hill et al. 2016</u> |
| <u>Mean watershed elevation</u> | <u>Basin Topography</u> | <u>m</u> | <u>Hill et al. 2016</u> |
| <u>Avg. stream slope</u> | <u>Basin Topography</u> | <u>mm⁻¹</u> | <u>Hill et al. 2016</u> |
| <u>Distance upstream</u> | <u>Basin Topography</u> | <u>km</u> | <u>Hill et al. 2016</u> |
| <u>% Watershed forest</u> | <u>Land Use</u> | <u>%</u> | <u>Hill et al. 2016; Dewitz et al. 2019</u> |
| <u>% Riparian forest</u> | <u>Land Use</u> | <u>%</u> | <u>Hill et al. 2016; Dewitz et al. 2019</u> |
| <u>% Lake area</u> | <u>Land Use</u> | <u>%</u> | <u>Hill et al. 2016; Dewitz et al. 2019</u> |
| <u>Avg. Temperature</u> | <u>Climate</u> | <u>C</u> | <u>Thornton et al. (2020)</u> |
| <u>Avg. Precipitation</u> | <u>Climate</u> | <u>mm</u> | <u>Thornton et al. (2020)</u> |
| <u>Avg. % precip as snow</u> | <u>Climate</u> | <u>%</u> | <u>Thornton et al. (2020)</u> |
| <u>Baseflow index</u> | <u>Hydrogeologic</u> | <u>%</u> | <u>Hill et al. 2016; Wolock 2003</u> |
| <u>Hydraulic conductivity</u> | <u>Hydrogeologic</u> | <u>%</u> | <u>Hill et al. 2016; Olson and Hawkins 2014</u> |
| <u>Soil depth to bedrock</u> | <u>Hydrogeologic</u> | <u>cm</u> | <u>Hill et al. 2016; Carlisle et al. 2009</u> |

Table 3. Air water correlation average summary metrics by basin and season. Averages are calculated as the mean value of summary metrics at all sites across each basin and season.

| | | Thermal Sensitivity | | | R ² | | |
|-------------------|---------------|---------------------|-------------|-------------|----------------|-------------|-------------|
| | | Min | Mean | Max | Min | Mean | Max |
| <u>Snoqualmie</u> | <u>Fall</u> | <u>0.22</u> | <u>0.59</u> | <u>0.79</u> | <u>0.58</u> | <u>0.92</u> | <u>0.99</u> |
| | <u>Winter</u> | <u>0.05</u> | <u>0.40</u> | <u>0.71</u> | <u>0.20</u> | <u>0.86</u> | <u>0.96</u> |
| | <u>Spring</u> | <u>0.26</u> | <u>0.60</u> | <u>0.97</u> | <u>0.67</u> | <u>0.89</u> | <u>0.98</u> |
| | <u>Summer</u> | <u>0.19</u> | <u>0.56</u> | <u>0.95</u> | <u>0.41</u> | <u>0.85</u> | <u>0.97</u> |
| <u>Wenatchee</u> | <u>Fall</u> | <u>0.40</u> | <u>0.57</u> | <u>0.74</u> | <u>0.74</u> | <u>0.94</u> | <u>0.98</u> |
| | <u>Winter</u> | <u>0.05</u> | <u>0.28</u> | <u>0.47</u> | <u>0.44</u> | <u>0.84</u> | <u>0.95</u> |
| | <u>Spring</u> | <u>0.14</u> | <u>0.42</u> | <u>0.72</u> | <u>0.59</u> | <u>0.88</u> | <u>0.98</u> |
| | <u>Summer</u> | <u>0.06</u> | <u>0.41</u> | <u>0.66</u> | <u>0.08</u> | <u>0.77</u> | <u>0.96</u> |

25

Table 4. Averaged metrics for all sites within each cluster determined with the spatially weighted agglomerative hierarchical clustering. For timing metrics, days are reported as hydrologic day, where a value of 1 indicates October 1st and a value of 365 indicates September 30th.

Formatted: Font: Bold

| Metric | Basin | Cluster | # Sites | Mean | Minimum (timing) | Maximum (timing) | Cluster Stability |
|------------------------|------------|---------|---------|------|---------------------|---------------------|----------------------|
| Thermal Sensitivity | Snoqualmie | 1 | 11 | 0.50 | 0.41 (224) | 0.56 (308) | 0.68 |
| | | 2 | 5 | 0.52 | 0.36 (181) | 0.81 (315) | 0.88 |
| | | 3 | 15 | 0.40 | 0.27 (201) | 0.64 (316) | 0.67 |
| | | 4 | 11 | 0.65 | 0.52 (199) | 0.84 (316) | 0.55 |
| | Wenatchee | 1 | 7 | 0.39 | 0.20 (216) | 0.65 (324) | 0.79 |
| | | 2 | 1 | 0.27 | 0.23 (28) | 0.30 (101) | 0.62 |
| | | 3 | 7 | 0.40 | 0.27 (131) | 0.54 (11) | 0.94 |
| | | 4 | 8 | 0.29 | 0.14 (207) | 0.48 (331) | 0.86 |
| | | 5 | 8 | 0.35 | 0.15 (214) | 0.66 (330) | 0.69 |
| Air | Snoqualmie | 1 | 31 | 10.2 | 1.01 (94) | 19.7 (305) | 0.91 |
| | | 2 | 11 | 8.02 | -0.42 (145) | 18.9 (304) | 0.73 |
| | Wenatchee | 1 | 6 | 9.68 | -4.52 (95) | 25.0 (304) | 0.95 |
| | | 2 | 25 | 6.48 | -7.88 (107) | 21.3 (310) | 0.85 |
| Water | Snoqualmie | 1 | 25 | 10.1 | 3.91 (94) | 17.8 (304) | 0.65 |
| | | 2 | 17 | 7.99 | 2.94 (94) | 15.6 (304) | 0.89 |
| | Wenatchee | 1 | 8 | 8.39 | 1.95 (108) | 18.5 (310) | 0.73 |
| | | 2 | 23 | 5.74 | 0.37 (107) | 14.5 (310) | 0.86 |

Page 38: [1] Deleted **Lillian McGill** **11/28/23 7:02:00 PM**

Page 39: [2] Deleted **Lillian McGill** **11/28/23 7:04:00 PM**